

AD 789127

Contributing to a better understanding of the environment



TECHNICAL REPORT NO. 71-22
ALASKAN NOISE FIELD INVESTIGATION,
MARCH TO JUNE 1971

APPROVED FOR PUBLIC RELEASE
DISTRIBUTION UNLIMITED

Details of illustrations in
this document may be better
studied on microfiche

D D C
RECORDED
MAR 7 1972
R LUGGILL
C

 **TELEDYNE
GEOTECH**

R
54

Unclassified

Security Classification

DOCUMENT CONTROL DATA - R & D

(Security classification of title, body of abstract and indexing annotation must be entered when the overall report is classified)

1. ORIGINATING ACTIVITY (Corporate author) Teledyne Geotech 3401 Shiloh Road Garland, Texas	2a. REPORT SECURITY CLASSIFICATION Unclassified
	2b. GROUP

3. REPORT TITLE
**Alaskan Noise Field Investigation,
March to June 1971**

4. DESCRIPTIVE NOTES (Type of report and inclusive dates)
Special investigation

5. AUTHOR(S) (First name, middle initial, last name)
Staff

6. REPORT DATE 17 January 1972	7a. TOTAL NO. OF PAGES 55	7b. NO. OF REFS 2
--	-------------------------------------	-----------------------------

8a. CONTRACT OR GRANT NO F33657-70-C-0646 b. PROJECT NO Project VT/0703 c. d.	9a. ORIGINATOR'S REPORT NUMBER(S) Technical Report No. 71-22
	9b. OTHER REPORT NO(S) (Any other numbers that may be assigned this report)

10. DISTRIBUTION STATEMENT
**Approved for Public Release.
Distribution Unlimited.**

11. SUPPLEMENTARY NOTES None	12. SPONSORING MILITARY ACTIVITY Advanced Research Projects Agency Nuclear Monitoring Research Office 1400 Wilson Blvd., Arlington, Va., 22209
--	--

13. ABSTRACT

Noise in the 50-60 second period range, recorded by the Alaskan Long-Period Array during the winter months, was found to be caused by convection cells within the array boreholes. A technique for preventing formation of the cells was devised.

Burial of ALPA seismometers was found to significantly reduce wind-generated horizontal seismic noise.

Relationships between triaxial module pressure sensitivities and module installation techniques and between pressure sensitivity and module tilt were studied.

Details of illustrations in this document may be better studied on microfiche

Unclassified

Security Classification

14	KEY WORDS	LINK A		LINK B		LINK C	
		ROLE	WT	ROLE	WT	ROLE	WT
	Long-period noise Long-period triaxial seismometers						

Unclassified

Security Classification

TECHNICAL REPORT NO. 71-22
ALASKAN NOISE FIELD INVESTIGATION,
MARCH to JUNE 1971

Sponsored by

Advanced Research Projects Agency
Nuclear Test Detection Office
ARPA Order No. 1714

Neither the Advanced Research Projects Agency nor the Air Force Technical Applications Center will be responsible for information contained herein which has been supplied by other organizations or contractors, and this document is subject to later revisions as may be necessary. The views and conclusions presented are those of the authors and should not be interpreted as necessarily representing the official policies, either expressed or implied, of the Advanced Research Projects Agency, the Air Force Technical Applications Center, or the U.S. Government.

Approved for Public Release.
Distribution Unlimited.

TELEDYNE GEOTECH
3401 Shiloh Road
Garland, Texas

17 January 1972

IDENTIFICATION

AFTAC Project No. VT/0703

Project Title: Long-Range Seismic Measurements

ARPA Order No. 624

ARPA Code No. 8F10

Contractor: Teledyne Geotech

Contract No. F33657-70-C-0646, Amendment 4

Program Manager: R.G. Roakes (214) 27-12561, ext. 230
Garland, Texas 75041

CONTENT

	<u>Page</u>
ABSTRACT	
1. INTRODUCTION	1
1.1 General	1
1.2 Authority	1
2. TEST AT ALPA SITE 3-3	1
2.1 Pressure pulse test with triax rotation	1
2.2 Borehole casing evacuation	2
2.3 Borehole pressure measurements	3
2.4 Borehole temperature measurements	6
2.5 The triax stiffening package	7
2.5.1 Tests with the unsealed stiffening package	7
2.5.2 Tests with the sealed stiffening package	10
3. ANALYSIS OF DATA FROM SITE 3-3	11
3.1 Spectral analysis of the noise at site 3-3	11
3.2 Pressure disturbances inside the casing	11
3.3 Noise reduction in ALPA boreholes	23
4. TESTS AT OTHER LOCATIONS	31
4.1 Tests at ALPA site 3-34	31
4.2 Vault installation at ALPA site 2-3	31
4.3 Tests at the ALPA monitor and maintenance center (MMC)	34
4.4 Tests at Garland, Texas	34
5. CONCLUSIONS AND RECOMMENDATIONS	37
APPENDIX 1 - Summary of triaxial seismometer tests at Fairbanks, Alaska, ALPA site 3-3	
APPENDIX 2 - Responses of triaxial seismometer modules to pressure pulses	
APPENDIX 3 - Summary of triaxial seismometer tests at ALPA site 3-34	

ILLUSTRATIONS

<u>Figure</u>		<u>Page</u>
1	Reproduction of 16 mm film from FB2AK, 13 April 1971. Dry ice was packed around the wellhead. The borehole sealed but not insulated	4
2	Reproduction of 16 mm film from FB2AK, 15 April 1971. The borehole was sealed and completely filled with insulation, and dry ice was packed around the wellhead	5
3	Installation of the triaxial seismometer stiffening package	8
4	Installation of stiffened triaxial seismometer package in borehole at site 3-3	9
5	Power density spectra of outside (MKB1) and inside (MKB2) microbarographs	12
6	Power density spectra of individual triax seismographs, TR1, TR2, and TR3. Dry ice packed around wellhead	13
7	Coherence and phase of the TR1 and TR2 seismograph. Dry ice packed around wellhead	14
8	Coherence and phase angle obtained from cross correlating the inside microbarographs (MKB2) and triax seismograph (TR1). Dry ice packed around wellhead	15
9	Phase differences between triaxial modules and microbarograph (MKB2) (corrected for instrument response). Dry ice packed around wellhead	17
10	Response of triaxial modules to pressure changes. Data are corrected for instrument responses. Data taken with dry ice around wellhead and with insulation removed from top 3-feet of borehole	18
11	Power density spectrum (not corrected for response) of the noise on triaxial module TR3 during pump test	20
12	Coherence between the inside microbarograph and triaxial module TR2 during pump test	21
13	Power density spectrum of the noise on triaxial module TR2 during vacuum test	22

ILLUSTRATIONS, Continued

<u>Figure</u>		<u>Page</u>
14	Spectra of the noise recorded by the surface vertical (LPZ) and the coordinate transformed vertical (ZCT) seismographs. Wind velocity 5.0 meters/sec	24
15	Theoretical vertical (W) and horizontal (U) surface displacement caused by pressure variations for a wind velocity (C) of 5 meters/sec	25
16a	Noise coherence between the east-west surface (LPE) and downhole (ECT) seismographs	27
16b	Noise coherence between vertical surface (LPZ) and downhole (ZCT) seismographs. Wind 5.0 meters/sec	27
17	Spectra of the noise recorded by the surface horizontal (LPN) and the coordinate transformed horizontal seismographs. Wind velocity is 5 meters/sec	28
18	Theoretical apparent horizontal displacements caused by ground tilt at the free surface	29
19	Theoretical attenuation of vertical displacements and tilts with depth	30
20	Special tank vault for subsurface installation at ALPA site 2-3	32
21	Cross-section of wellhead vault installation at ALPA site 2-3	33
22	Pressure sensitivity of triaxial seismometer module as a function of module tilt. Free period adjusted to 20 ± 0.5 sec for each data point	35
23	Pressure sensitivity of triaxial seismometer module as function of module free period	36

ABSTRACT

Noise in the 50-60 second period range, recorded by the Alaskan Long-Period Array during the winter months, was found to be caused by convection cells within the array boreholes. A technique for preventing formation of the cells was devised.

Burial of ALPA seismometers was found to significantly reduce wind-generated horizontal seismic noise.

Relationships between triaxial module pressure sensitivities and module installation techniques and between pressure sensitivity and module tilt were studied.

ALASKAN NOISE FIELD INVESTIGATION,
MARCH TO JUNE 1971

1. INTRODUCTION

1.1 GENERAL

Early in March 1971, the Project Office issued a detailed plan for conducting a series of tests on some of the triaxial seismometers used in the Alaskan Long-Period Array (ALPA) near Fairbanks, Alaska. The purpose of these tests was to determine the source of the 50-60 second noise recorded by the ALPA during the winter months and to eliminate this noise source. The plan required that work be performed at ALPA sites 3-3 and 3-4 and LRSM site FB2AK, and called for the performance of the maximum number of tests before the noise subsided in the spring. Unfortunately, this happened only a few days after tests were begun, requiring that the test plan schedule be modified, but work was continued until mid-June.

1.2 AUTHORITY

All work was performed under the authorization of task d of Contract F33657-70-C-0646, and with the prior approval of the Project Officer.

2. TEST AT ALPA SITE 3-3

Tests, conducted at site 3-3, from early March to mid-June, closely followed the test plan, and were directed toward determining the relationship between winter noise and pressure changes in the borehole. Later tests were performed to collect data which would lead to an understanding of the mechanism by which the triaxial seismometer responded to pressure changes. Details of work undertaken and results of tests at this site are listed chronologically in appendix 1.

2.1 PRESSURE PULSE TEST WITH TRIAX ROTATION

Previous work showed that pressure pulses, applied to a borehole, caused all triaxial modules to produce outputs with the same phase relationship as they did for winter noise. That is, if the module outputs indicated that the winter noise was propagating from the north, they also indicated that the pressure pulses appeared to propagate from the north. Although that early work was hurriedly performed under poorly-controlled conditions, it strongly suggested that the noise was, in some way, related to pressure changes. Therefore, the previous work was repeated at ALPA site 3-3 under carefully controlled conditions. A tire pump was modified to produce 0.5 millibar step pressure

pulses in the sealed borehole, and the triaxial modules were subjected to these pulses when oriented normally, rotated 120° from normal, and rotated 240° from normal.

Appendix 2 presents a consolidated tabulation of the results of the pressure pulse tests with all readings reduced to equivalent ground motion in microns. Note that the 8 and 11 March data show that the polarity of the module pressure sensitivity is related to module orientation in the borehole. Another observation that related triaxial module responses to their orientation in borehole was made by the on-site personnel, who found that the phase and amplitude relationships of the recorded pulse data made the pulses appear to propagate from a specific azimuth, the same one from which winter noise appeared to propagate.

The 13 through 23 May data show that mounting the triaxial modules in a stiffener removes the apparently directionality of the pressure pulse responses, and the 6 through 12 June data show that dependence of module pressure sensitivity upon module stack orientation and upon type of stack support is greatly reduced by sealing the stiffener. The stiffener is discussed in greater detail in section 2.5.

2.2 BOREHOLE CASING EVACUATION

On 17 March, the average ambient temperature at the site rose from -25°C (-15°F) to -10°C (+15°F), and the winter noise recorded by the triaxial seismograph faded away. It reappeared several times when the ambient temperature dropped but not at the high amplitudes nor at the long intervals recorded during the winter months. The appearance and disappearance of this noise was not always clearly discernable, as strong winds blew throughout March and generally increased the recorded background noise.

At that time, it was suggested that the noise sensed by the triaxial seismograph might be caused by pressure changes within the borehole which, in turn are caused by convection cells. This theory was based on three observations: 1) that the triaxial modules are sensitive to pressure changes, 2) that amplitudes of microbarometric noise in the borehole are directly related to amplitudes of triaxial seismograph noise, and 3) that both are inversely related to ambient temperature. Furthermore, it was suggested that the convection cells might be caused by temperature inversions at the wellhead because the temperature there varied greatly, staying within $\pm 1^\circ\text{C}$ of the outdoor air temperature while the temperature at the bottom of the hole remained constant at $2.90 \pm 0.01^\circ\text{C}$. It was thought that if this theory were accurate, it should be possible to generate noise inside a sealed, air-filled borehole by cooling the wellhead. Conversely, it should not be possible to generate noise by cooling the wellhead of an evacuated borehole.

The theory was tested at site 3-3, where data were taken with the borehole both evacuated and air-filled. Two methods were used to cool the wellhead. In one, the wellhead was packed with dry ice. In the other, the wellhead was exposed to the environment and was cooled each night as the air temperature fell. No significant (50-60 second) noise was sensed by the triaxial modules when the

borehole was evacuated to 4 torr and the wellhead was allowed to cool overnight. When air was allowed to enter the borehole, and the wellhead was packed with dry ice, large amplitude noise was observed. The borehole was then evacuated with the dry ice continuing to cool the wellhead. Recorded noise was found to decrease as borehole air pressure decreased and became indiscernable at a vacuum of 20 torr.

2.3 BOREHOLE PRESSURE MEASUREMENTS

On 10 April, a microbarograph (MKB2) was placed into operation to sense pressure changes inside and near the top of the sealed borehole. The transducer was installed inside a sealed tank vault to isolate the unit from outside pressure changes. When MKB2 went into operation, it was immediately apparent that a large part of the triaxial seismograph noise was caused by pressure changes inside the borehole. Noise in the outputs from the three triaxial modules and the microbarograph showed a high degree of correlation.

Also on 10 April, a thermistor was placed inside the borehole near the top and relative temperature data from its bridge circuit were recorded on the same film that recorded triaxial seismograph and MKB2 outputs. The data showed that 50-60 second noise outputs from the MKB2 and all three seismograph channels increased as the borehole temperature decreased. Dry ice was packed around the wellhead on 13 April and the pressure noise inside the well was very high. On 14 April, the borehole was opened and was completely filled to the top with crumbled polystyrene. The well was sealed and dry ice was again packed around the wellhead. Figures 1 and 2 are samples of typical data recorded with dry ice on the wellhead before and after the polystyrene was installed. Note that although the MKB2 channel magnification is 12 dB higher in figure 2 than in figure 1, no pressure changes were detected in the insulated borehole. None were detected even when the gain of the MKB2 channel was increased until the microbarograph system noise could be seen.

The success in decreasing seismograph noise by filling the borehole with polystyrene raised the question as to why this technique had been unsuccessful during earlier tests when the winter noise level was high. It was learned that in these earlier tests, the borehole had not been completely filled, that about 3 feet of open space had been left at the top. To determine if this was significant, about 3 feet of polystyrene was removed from the borehole and dry ice was packed around the sealed wellhead. The microbarograph channel showed an increase in noise to a level comparable to that recorded when similar tests were made with the borehole uninsulated.

Data from foregoing series of borehole pressure and temperature measurements led to the following conclusions:

- a. Relatively large pressure variations can be produced in a sealed borehole by convection cells near the top of the hole.
- b. The triaxial seismometer responds to pressure changes.

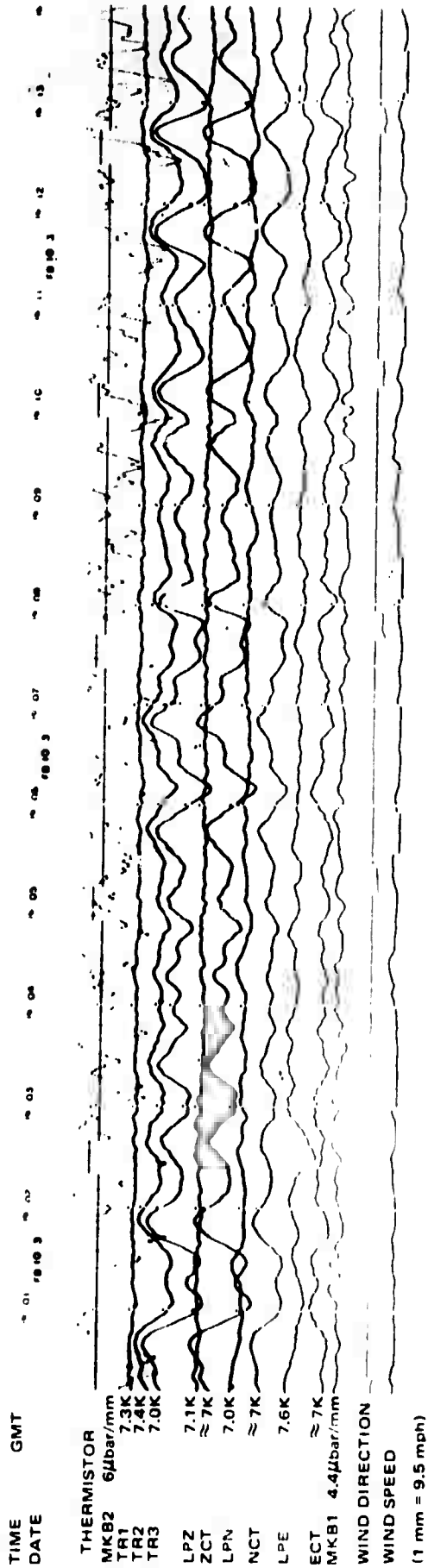


Figure 1. Reproduction of 16 mm film from FB2AK, 13 April 1971. Dry ice was packed around the wellhead. The borehole sealed but not insulated

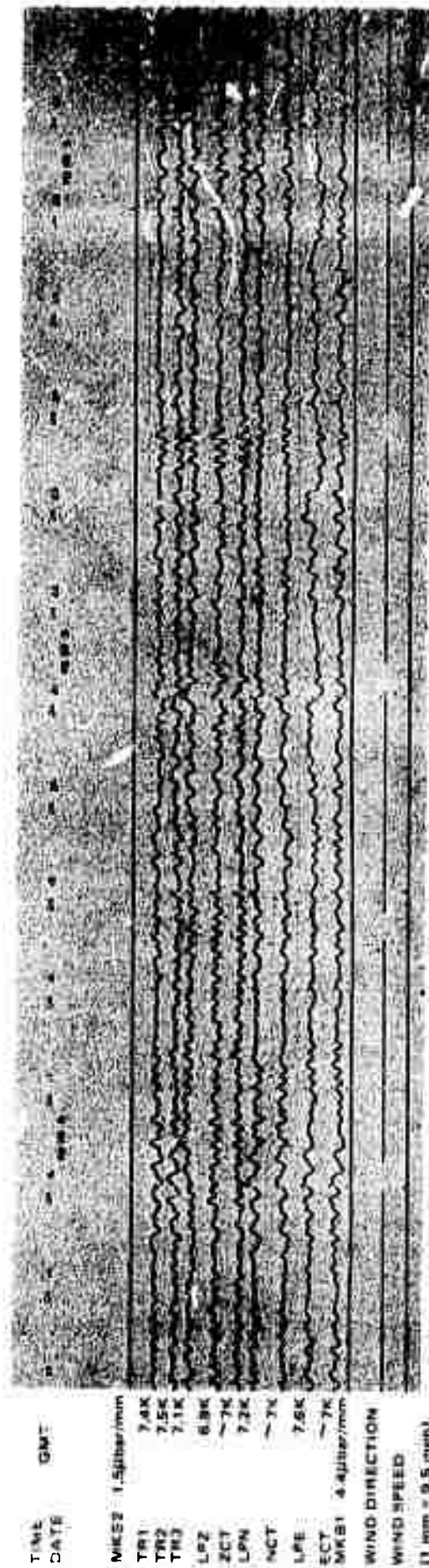


Figure 2. Reproduction of 16 mm film from FB2AK, 15 April 1971. The borehole was sealed and completely filled with insulation, and dry ice was packed around the wellhead

c. Pressure changes within the sealed borehole are not related to ambient pressure changes.

d. The noise sensed during the winter months by the triaxial seismometers at ALPA probably is caused by pressure changes inside the borehole due to the convection of air inside the casing, which in turn is caused by an air column that is colder at the top than it is at the bottom.

e. Convection cells, large enough to produce pressure changes that can be sensed by a triaxial seismometer, can be prevented from forming by completely filling the borehole with a baffling material such as crumbled polystyrene foam.

2.4 BOREHOLE TEMPERATURE MEASUREMENTS

A differential thermometer, designed and tested during May, was used to measure variations in the difference between temperatures at two points 1 meter apart. The thermometer used two thermistors to sense temperatures, a bridge circuit to compare thermistor resistances, and a phototube amplifier (PTA) to amplify and filter the bridge output. This unit had a resolution of 0.001°C and a pass band of 10 to 100 seconds.

The thermistor sensor assembly was installed near the top of the triaxial seismometer in the borehole at site 3-3, and differential temperature data were recorded on Develocorder film with triaxial seismograph data. This was done on 13 May, just after the seismometer was reinstalled following maintenance, and with no polystyrene in the borehole. Variations in differential temperature were about 0.01°C p-p when measurements were begun, but decreased to about 0.002°C p-p 10 hours later.

Twenty-four hours after installation, the differential temperature decreased to less than 0.001°C p-p, and remained at this level until the channel operation was terminated on 21 May. Seismograph noise subsided during the same time period. These data indicate that the act of installing the triaxial seismometer disturbed the thermal equilibrium of the borehole and caused the formation of at least one convection cell that generated noise. In this case, it appears that convection caused air motion in the vicinity of the seismometer.

To determine if noise in the seismometer output could be caused by this air motion rather than by the pressure changes in the borehole, a series of 0.5 millibar pressure pulses were applied to the top of the sealed borehole, and then, dry ice was placed about the wellhead. The pressure pulses produced differential temperature variations of about 0.001°C at the seismometer, and the dry ice produced no differential temperature variations that could be correlated with the noise recorded on the seismograph channel, indicating that neither action caused significant air motion near the seismometer.

These test results show that triaxial seismograph noise is not caused by air convection near the seismometer, but rather is caused by pressure changes acting upon the instrument.

2.5 THE TRIAX STIFFENING PACKAGE

After pressure changes inside the borehole were identified as the source of winter noise on triaxial seismometer, work that followed was directed toward gaining an understanding of the mechanism that produces these pressure changes. Because results of earlier tests suggested that the seismometer assembly might be flexing in response to pressure changes, the seismometer construction was reviewed. The overall assembly was visualized as a vertical column supported at its bottom and horizontally constrained only at its top and bottom. It appeared possible that the unconstrained middle portion of the assembly could be flexed by unbalanced column loading caused by pressure on the top of the stack.

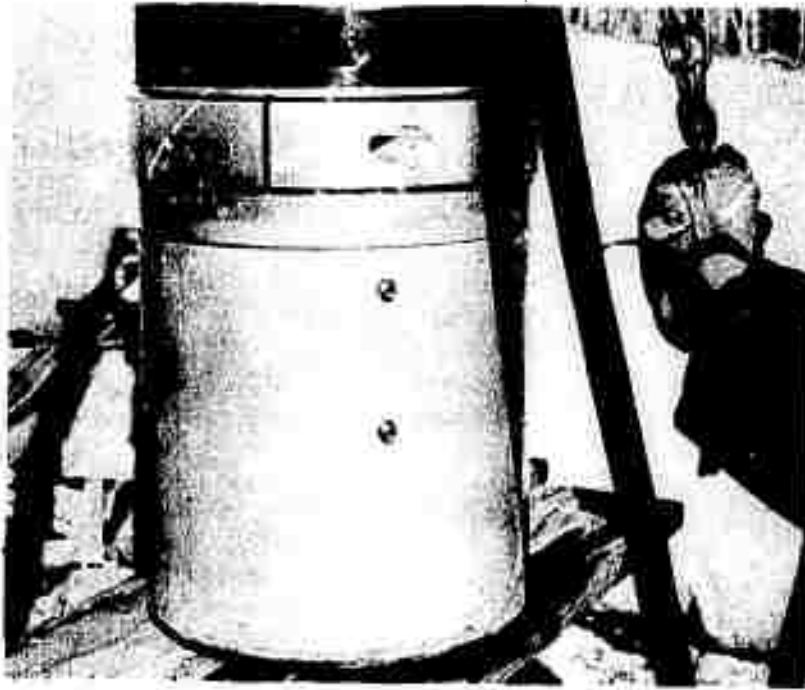
At the direction of the Project Officer, a stiffening package for the triaxial seismometer was designed and built in April. An external stiffening package was used to encase the entire triaxial seismometer because it could be built quickly and economically, and because it could be used without modifying the seismometer. The package was designed to stiffen the seismometer assembly rather than to isolate it from pressure changes, and was made from eight feet of 11-3/4 inch o.d. API schedule J-55 steel casing, which has a wall thickness of about 0.4 inch, and weighs about 400 pounds. Calculations showed that this stiffening package was strong enough to restrain module displacement and tilt enough so that seismometer responses to typical borehole pressure changes (100-200 microbar p-p) would be below system noise levels.

The seismometer was attached to the tube with three aluminum split clamps which fit in the bolt clearance groove of the lower flange on each triaxial module. Shims were used between the stabilizer and holelock units and the stiffening package to center the seismometer and to prevent its deformation. A domed cap was bolted to the bottom of the stiffening package. This evenly distributed the load on the package when it was operated on the bottom of the borehole.

The stiffening package was installed on the seismometer at site 3-3 between 4 and 12 May. Figures 3 and 4 are photographs taken during the installation.

2.5.1 Tests with the Unsealed Stiffening Package

Between 13 to 28 May, several tests were performed with the seismometer in its unsealed stiffening package. On 14 May, when dry ice was placed on the sealed wellhead, the internal microbarograph and the three triaxial module outputs became noisy and exhibited a high degree of visual correlation. During the remainder of this time, the stiffened seismometer was operated in several different configurations: on the bottom of the hole; supported by the holelock and stabilizer; supported by the holelock alone; and rotated through a full circle in 120° increments. Pressure pulse tests were performed for each configuration.

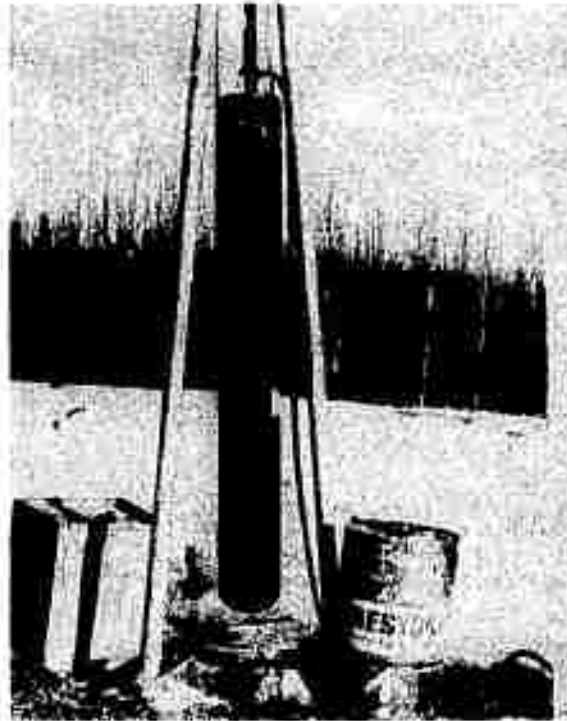


- a. View showing installation of holelock complete and lowest split clamp in place on bottom triaxial module. Ready to lower seismometer into stiffener tube



- b. Installing highest split clamp and lowering seismometer into tube

Figure 3. Installation of the triaxial seismometer stiffening package



a. Installation of stiffening package complete. Note clearance holes in top and bottom for stabilizing plunger and holelock cam, respectively



b. Lowering package into borehole

Figure 4. Installation of stiffened triaxial seismometer package in borehole at site 3-3

G 6485

Results of the tests with the unsealed stiffening package are as follows:

a. The unsealed stiffening package did not reduce the seismometer response to pressure pulses.

b. All three triaxial modules responded to pressure pulses with deflections of the same polarity regardless of the package orientation.

These results indicate strongly that pressure-induced intermodule flexing of the seismometer is not responsible for the instrument pressure sensitivity and suggest that earlier tests, which showed that the polarity and/or amplitude changed every time the seismometer was disturbed, were influenced by instrument malfunction or other uncontrolled factors.

2.5.2 Tests with the Sealed Stiffening Package

Since intermodule flexing did not appear to be the source of triaxial seismometer noise, it was concluded that pressure changes must act directly on the modules to produce the noise. To verify this, tests were run after an attempt was made to isolate the seismometer from direct pressure effects by sealing the stiffening package. All access holes, and the annular areas between the seismometer and the inside of the stiffener and near the top of the top module (TR3) and the bottom of the bottom module (TR1) were filled with a flexible sealing compound called RES-O-LYN. Mounting bolts were covered over with RES-O-LYN to seal them. Holelock and stabilizer functions were unaffected by the sealing. The seal was checked both before and after performance of tests through a pipe fitting installed in the side of the stiffener. No internal pressure change could be detected over a 24-hour period by a manometer that had a resolution of better than 0.1 inch of water. This is equivalent to a time constant of more than 240 hours. It should be noted that the seal did not isolate the top or the bottom of the seismometer from pressure changes, but greatly reduced pressure acting radially upon the triax cases. Prior to sealing the stiffener, the pressure seal of each module was checked through pipe fittings installed in the Fiberglas module cases. Modules TR1 and TR2 had time constants greater than 24 hours when first tested, but TR3 required repairs before attaining that time constant.

The sealing work was accomplished between 29 May and 5 June. Tests with the sealed package began immediately thereafter and continued until 12 June. They consisted primarily of the application of pressure pulses to the borehole with the package oriented and supported in the same manner as it was during the tests run when the stiffener was unsealed.

Recorded data showed that during 5 of the 6 pressure pulse tests, the TR1 (bottom) and TR2 (middle) modules produced negative outputs while the TR3 (top) module produced a positive output in response to each positive pressure pulse. Note that, when these tests were run with the stiffening package unsealed, all outputs were negative. Furthermore, the middle module (TR2) produced consistently lower amplitude outputs than it did for any previous pulse test.

It is interesting to note that the sealed stiffening package appears to constrain the seismometer without reducing its pressure sensitivity.

5. ANALYSIS OF DATA FROM SITE 3-3

3.1 SPECTRAL ANALYSIS OF THE NOISE AT SITE 3-3

Analysis of the data recorded at site 3-3 of ALPA was done with limited objectives in mind. The principal task was to determine the cause of the long-period high-amplitude noise prevalent during the winter. Until the return of winter, it is not possible to be sure that the cause has been found; however, it appears almost certain that convection currents initiated by large temperature gradients at the top of the casing are basically responsible for the noise.

Another area, the attenuation of atmospherically-generated noise, was examined in much less detail.

Almost all of the analysis was performed using untransformed triaxial outputs. Because it was believed that earth motion did not cause the long-period noise, it was decided that the transformed time series might obscure the relative behavior of the three modules and thus make understanding the phenomenon more difficult.

Because of our interest in the longer periods, the antialiasing low-pass filter was set at 10-second period for all the spectra represented.

A number of spectra that were computed are not discussed in the report because no meaningful conclusions could be drawn from these results.

3.2 PRESSURE DISTURBANCES INSIDE THE CASING

A microbarograph was installed at site 3-3 to determine if pressure variations were present inside the casing. At the time this microbarograph was installed, the noise associated with the freezing temperatures of the winter months was no longer present; therefore, it was decided to simulate winter conditions by putting dry ice around the top of the casing, as the data revealed that it was possible to excite convection currents in the casing in this fashion. The phenomenon took place despite the fact that the casing was filled with expanded polystyrene to within 3 feet of the top of the casing.

Visually, there was a high correlation between the individual triaxial seismograms and the microbarograph records of pressure variations inside the casing. Figures 5 through 8 show the results obtained from analyzing typical background noise recorded when the convection cells were induced by dry ice. These results have not been corrected for seismograph or microbarograph amplitude response.

3600 SAMPLES, 256 LAGS, 1.0 SPS, PARZEN SMOOTHING
FB2AK
25 APRIL 1971
0110/0210

♦ MKB1
* MKB2

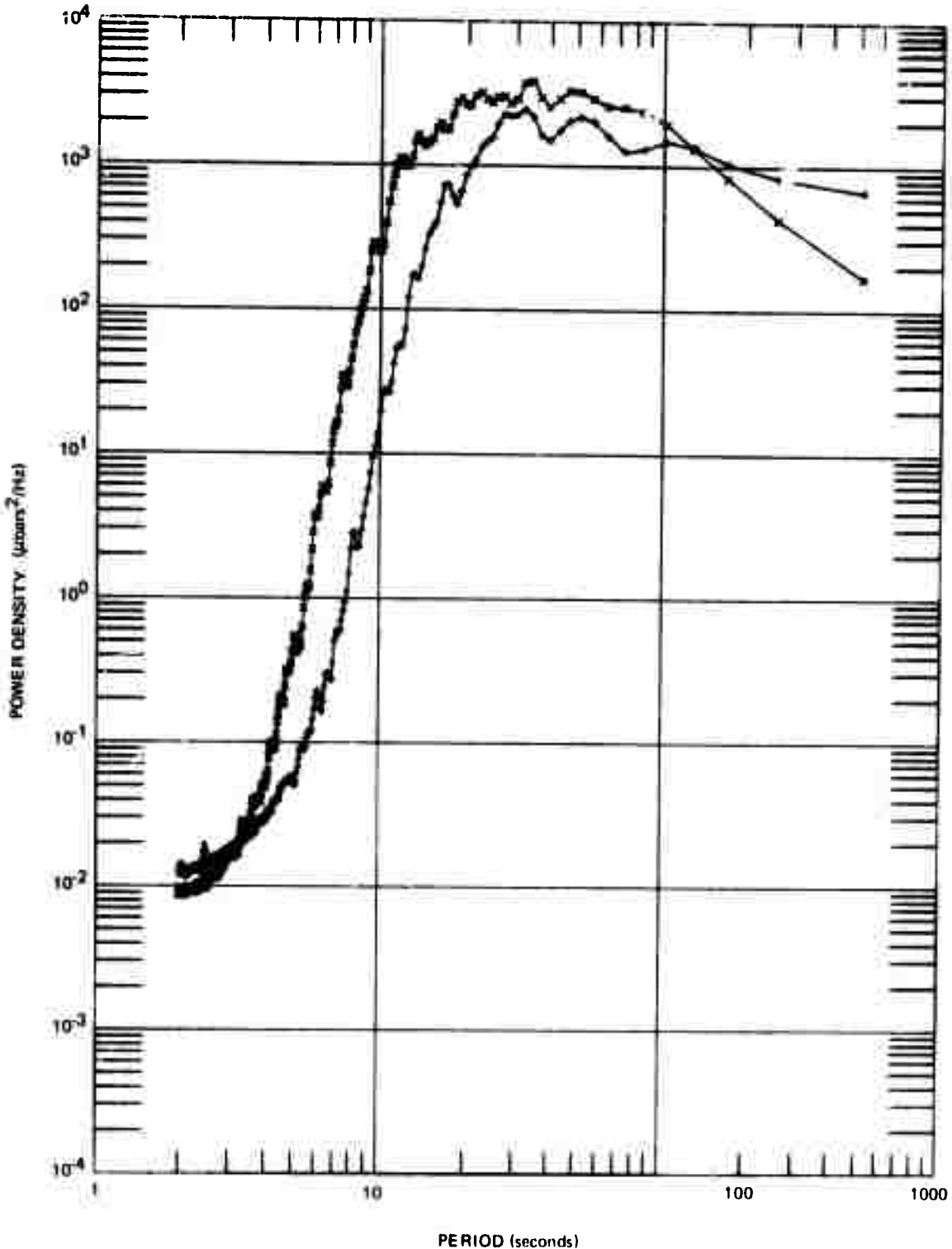


Figure 5. Power density spectra of outside (MKB1) and inside (MKB2) microbarographs

3600 SAMPLES, 256 LAGS, 1.0 EPS, PARZEN SMOOTHING
FB2AK
25 APRIL 1971
0110/0210

♦ TR1
× TR2
● TR3

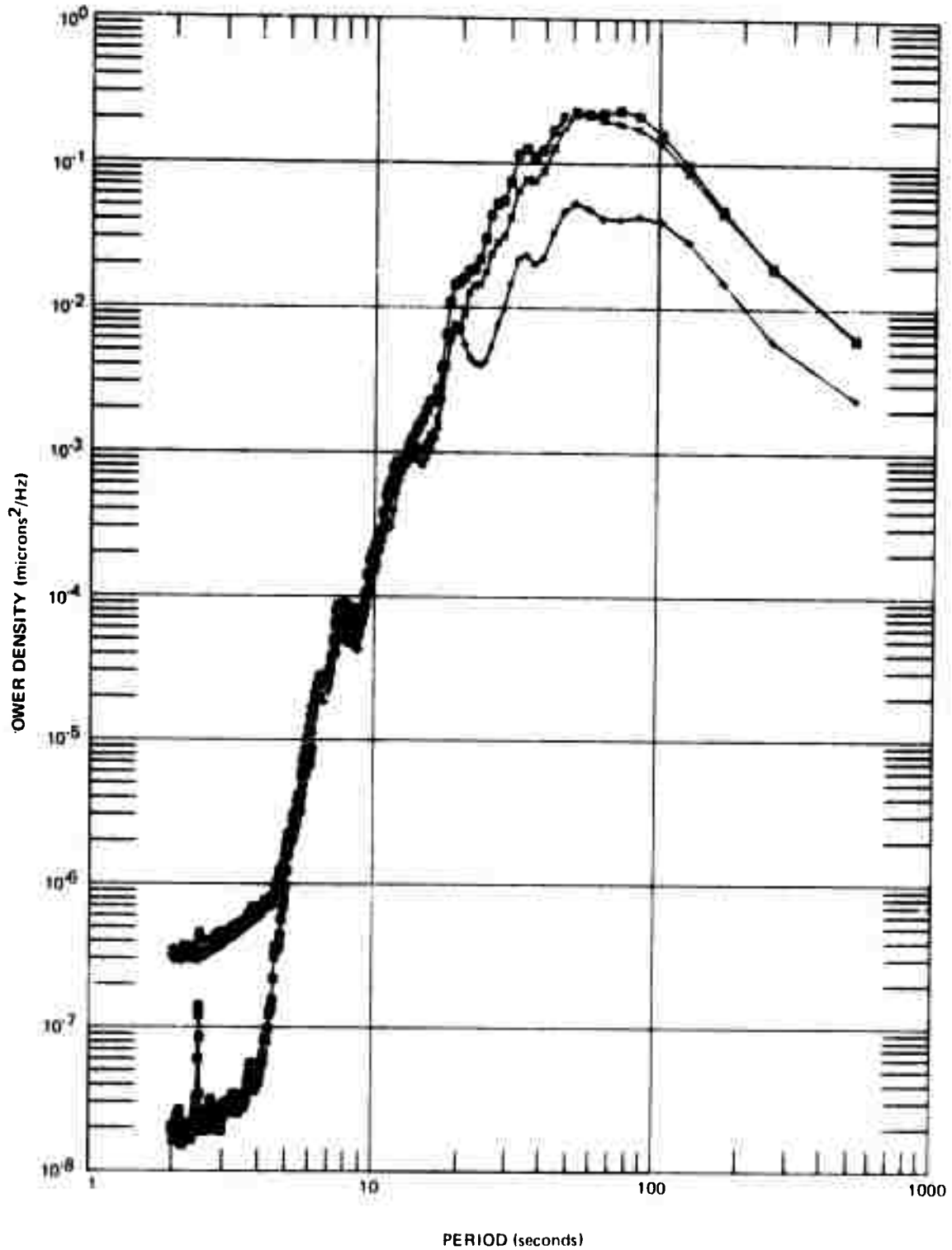
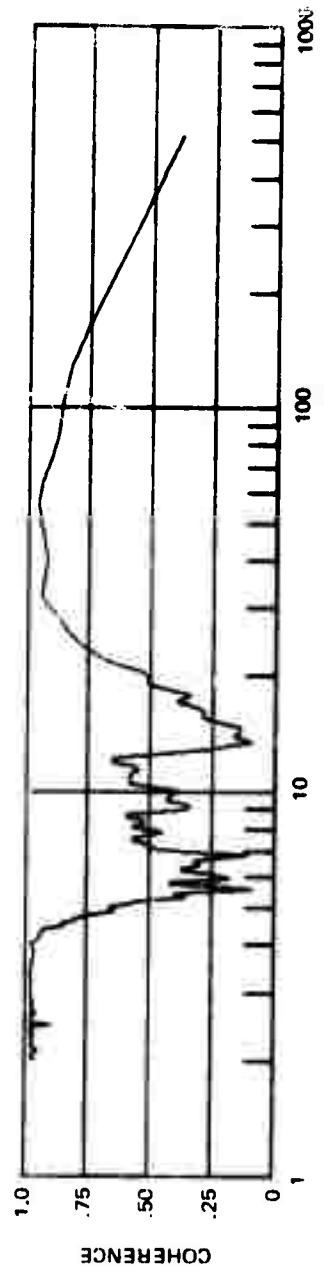


Figure 6. Power density spectra of individual triax seismographs, TR1, TR2, and TR3. Dry ice packed around wellhead

COHERENCE

3600 SAMPLES, 256 LAGS, 1.0 SPS, PARZEN SMOOTHING
TRI X TR2

FB2AK
25 APRIL 1971
0110/0210



PHASE

3600 SAMPLES, 256 LAGS, 1.0 SPS, PARZEN SMOOTHING
TRI X TR2

FB2AK
25 APRIL 1971
0110/0210

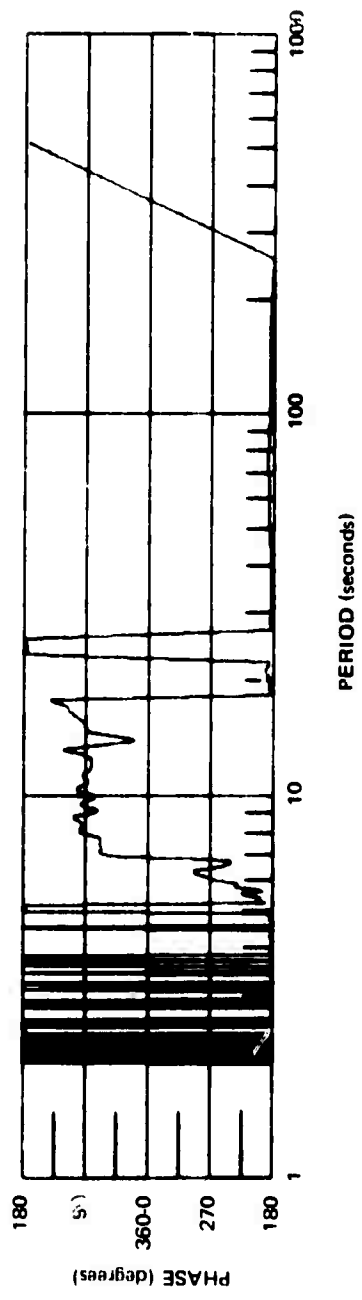
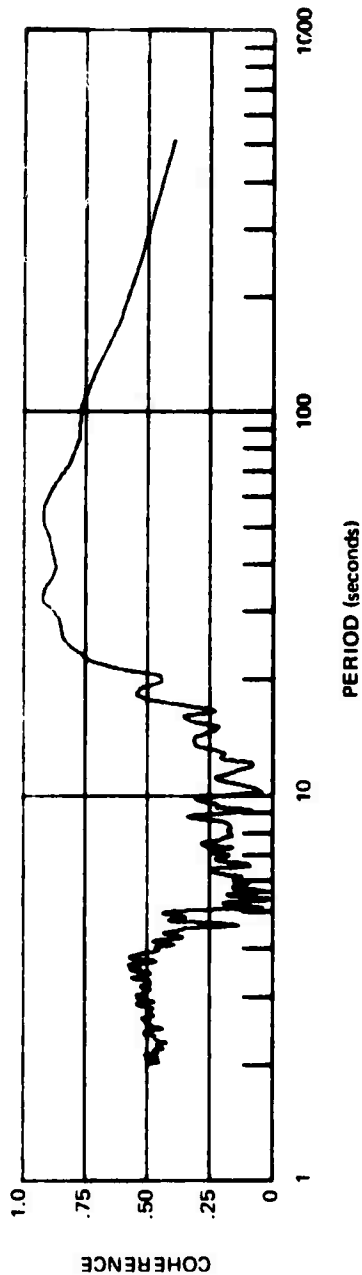


Figure 7. Coherence and phase of the TR1 and TR2 seismograph. Dry ice packed around wellhead

COHERENCE

3600 SAMPLES, 256 LAGS, 1.0 SPS, PARZEN SMOOTHING
TRI X MKB2

FBZAK
25 APRIL 1971
0110/0210



PHASE

3600 SAMPLES, 256 LAGS, 1.0 SPS, PARZEN SMOOTHING
TRI X MKB2

FBZAK
25 APRIL 1971
0110/0210

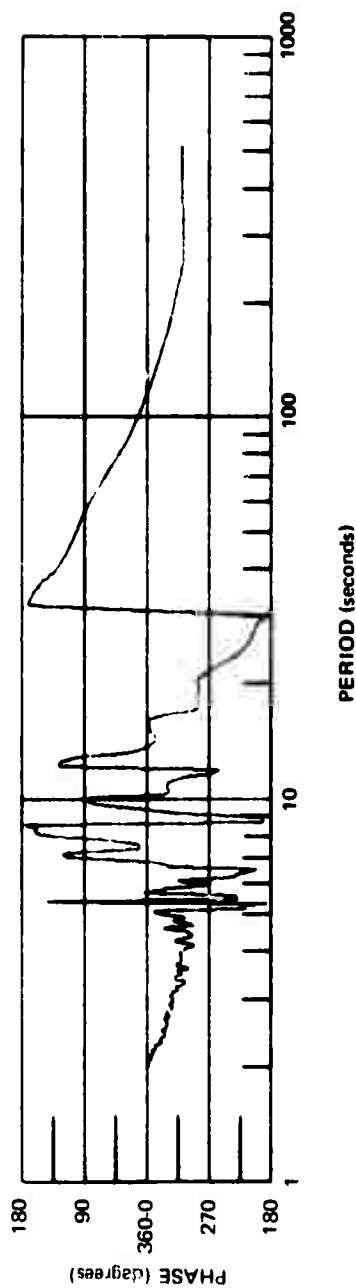


Figure 8. Coherence and phase angle obtained from cross correlating the inside microbarographs (MKB2) and triax seismograph (TRI). Dry ice packed around wellhead

Figure 5 shows the power spectra of data from the outside and inside microbarographs. Outside, or atmospheric pressure changes were recorded by MKB1. Inside, or borehole pressure changes were recorded by MKB2.

The power level of pressure changes inside the borehole was truly astonishing, but was real, as the instrument calibrations were verified by a number of tests. The coherence (not illustrated) between the two microbarographs was negligible, indicating that the inside pressure variations were not caused by atmospheric pressure variations. Therefore, leakage from the atmosphere into the casing is not the cause of the noise; furthermore, there was no relationship between the level of wind-generated noise outside and the pressure variations inside the casing. Figure 6 shows the power spectra of the individual triaxial seismograph traces peaking at the longer periods in the same general period range where the inside microbarograph peaks. The high coherence and the 0 to 180 degree phase shifts shown in figure 7 are very similar to the behavior of the triaxial seismograph during the winter, and suggest that the same mechanism is taking place. It appears from these results that the large temperature gradient (estimated to be more than 40°C per foot) produced at the wellhead during these tests, is capable of generating relatively high-velocity convection cells; a large temperature gradient is probably also present at the top of the casing during the winter months.

Figure 8 shows the coherence and the phase angles (uncorrected for system responses) obtained by cross-correlating the inside microbarograph with triaxial module TR1. The high coherence for periods less than 6.0 seconds is caused by analog tape noise. The coherence is extremely high in the period range of interest indicating a simple linear transfer function between the pressure variations inside the casing and the motion of the seismograph mass. In figure 9 the phase angles have been corrected for the theoretical phase responses of the two systems; the seismograph phase response is quite accurately known, the microbarograph response less accurately. Despite this uncertainty, there is a clear period-dependent phase shift. Buoyancy of the mass is not responsible; this would result in a 180 degree phase shift at periods above the natural period of the seismometer.

Figure 10 shows the response of the triaxial modules to pressure changes in millimicron per microbar (corrected for instrument responses). For the period range above 20 seconds, where the pressure-generated noise predominates, the triaxial module response to pressure increases very rapidly (approximately 12 dB/octave) towards the longer periods; it is approximately a straight line on the log-log plot.

The results given in figures 9 and 10 are the transfer function between the pressure variations recorded at the top of the casing and the mass motion of the triaxial modules. The results imply the presence of an efficient filter, either mechanical or acoustical. It may be that, at least partly, the filter action is caused by frequency-dependent absorption of the polystyrene in the casing. This transfer function can be calculated from the results discussed above and the noise eliminated by using an inside microbarograph and computing the expected seismograph motion. However, filling the casing with polystyrene is a far simpler solution to the problem.

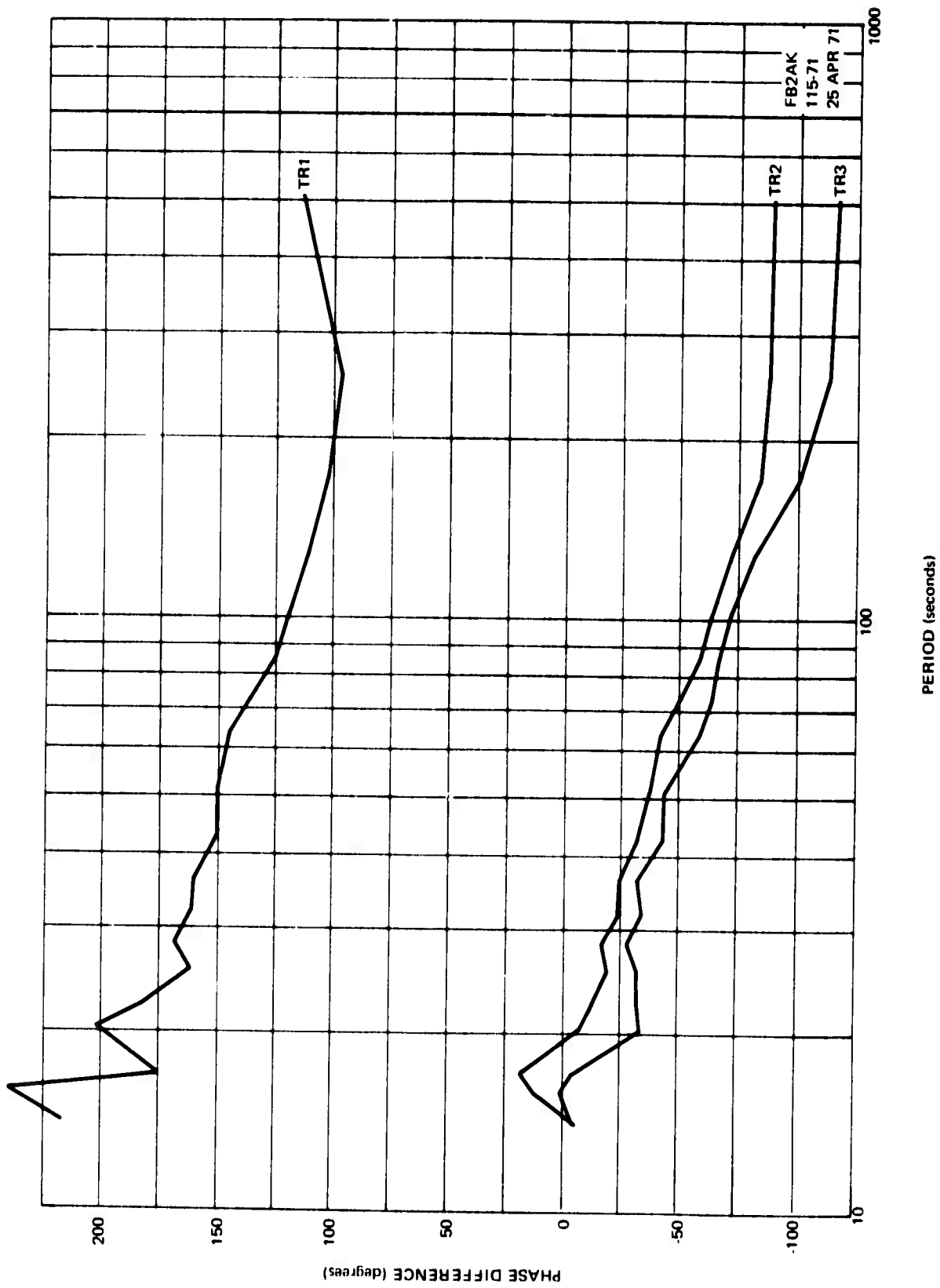


Figure 9. Phase differences between triaxial modules and microbarograph (MKB2) (corrected for instrument response). Dry ice packed around wellhead

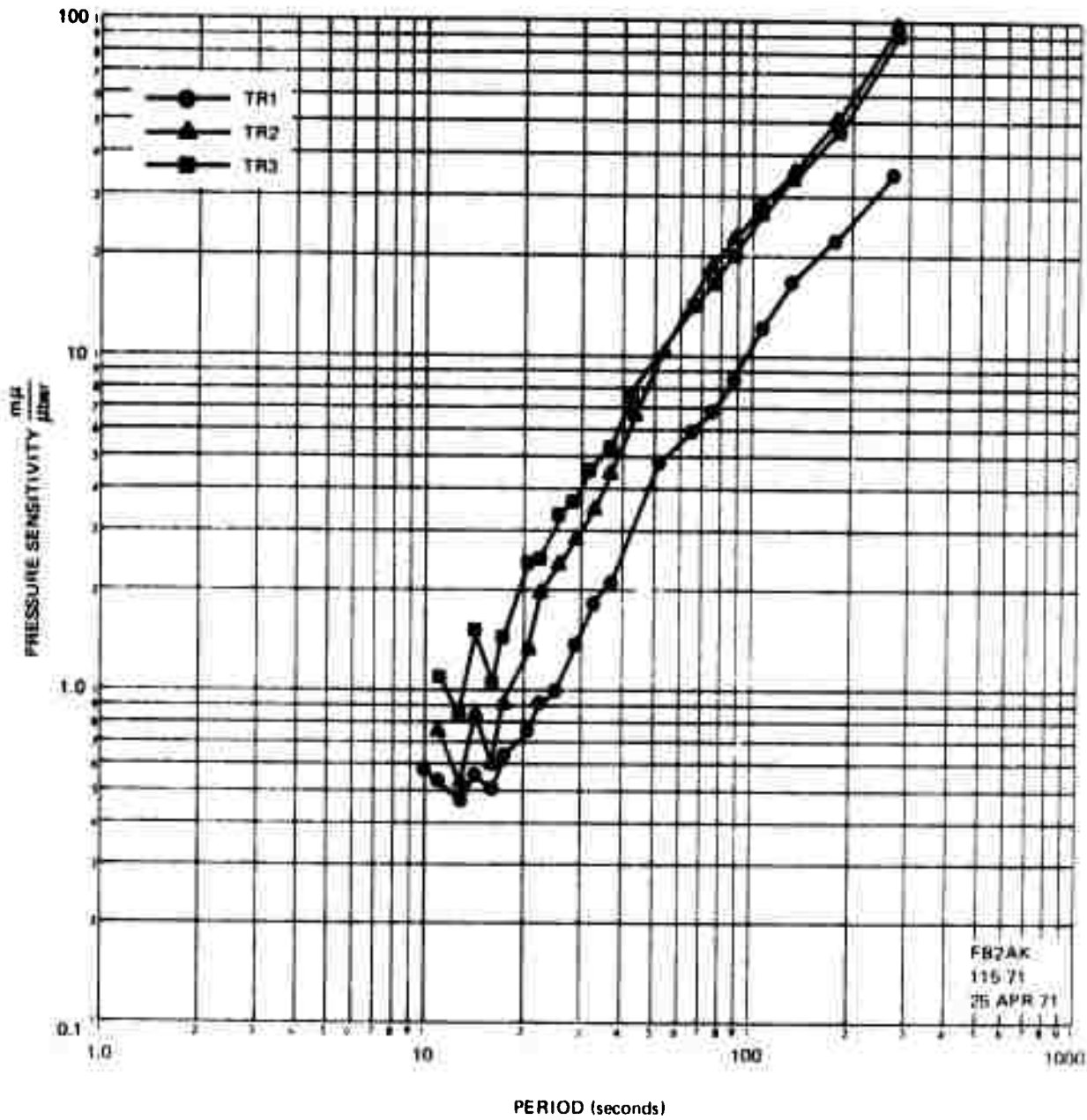


Figure 10. Response of triaxial modules to pressure changes. Data are corrected for instrument responses. Data taken with dry ice around wellhead and with insulation removed from top 3-feet of borehole

To further study the pressure sensitivity of the system, another test was run. A pressure pump was connected to the borehole and was used to introduce a 60-second period pressure variation into the borehole. Figures 11 and 12 shows the spectrum obtained from triaxial module TR2 and the coherence between this module and the inside microbarograph during this pressure test. The input was found to be not a pure sine wave; the side lobe energy caused by this non-linearity is clearly visible in the coherence values. The results obtained in this test verified the results from the convection current experiment as to the pressure sensitivity of the triaxial seismometer.

Figure 13 shows the spectrum of the noise recorded by module TR2 when the borehole was evacuated to 4.0 torr, and when there was little or no wind activity. As expected, a low level of energy was recorded at longer periods (>30 seconds) during this time. In fact, most of the energy at the period beyond 50 seconds consisted of system noise.

The results of these analysis do not indicate whether the pressure variations inside the casing move the seismometer by deforming the casing or whether they deform the seismometer assembly itself. To aid in determining which mechanism is acting, calculations of pressure-induced casing deformations were made. In these calculations, the pressure changes were assumed to occur so slowly that dynamic parameters could be ignored. Furthermore, it was assumed that the pressure changed uniformly over all surfaces within the casing, because pressure changes produced by convection cells at the top of the casing were propagated to all surfaces at acoustic velocities.

Therefore, the equations of static elasticity (Lamb, 1960)¹ were used to describe the radial motion (U_r) of the casing

$$U_r = \frac{bP}{E} \left[\frac{(1 + \nu) a^2 + b^2}{a^2 - b^2} - 2\nu b^2 \right]$$

where

P is the pressure inside the casing

E is Young's Modulus assumed to be 10^6 bars

a is the outside diameter of the casing, 13.375 in.

b is the inside diameter of the casing, 12.715 in.

ν is Poisson's Ratio assumed to be .25.

Using the formula and numbers given above, we compute the radial displacement caused by pressure variations for the limiting case when the cement is very poor, i.e., it is assumed to be entirely absent. The result is a radial displacement of 3×10^{-3} mm per μ bar.

¹ Lamb, Horace, 1960: Statics, Cambridge University Press, New York.

PUMP
1560 SAMPLES, 256 LAGS, 1.0 SPS, PARZEN SMOOTHING
FB2AK
4 MAY 1971
2121/2147
■ TR3

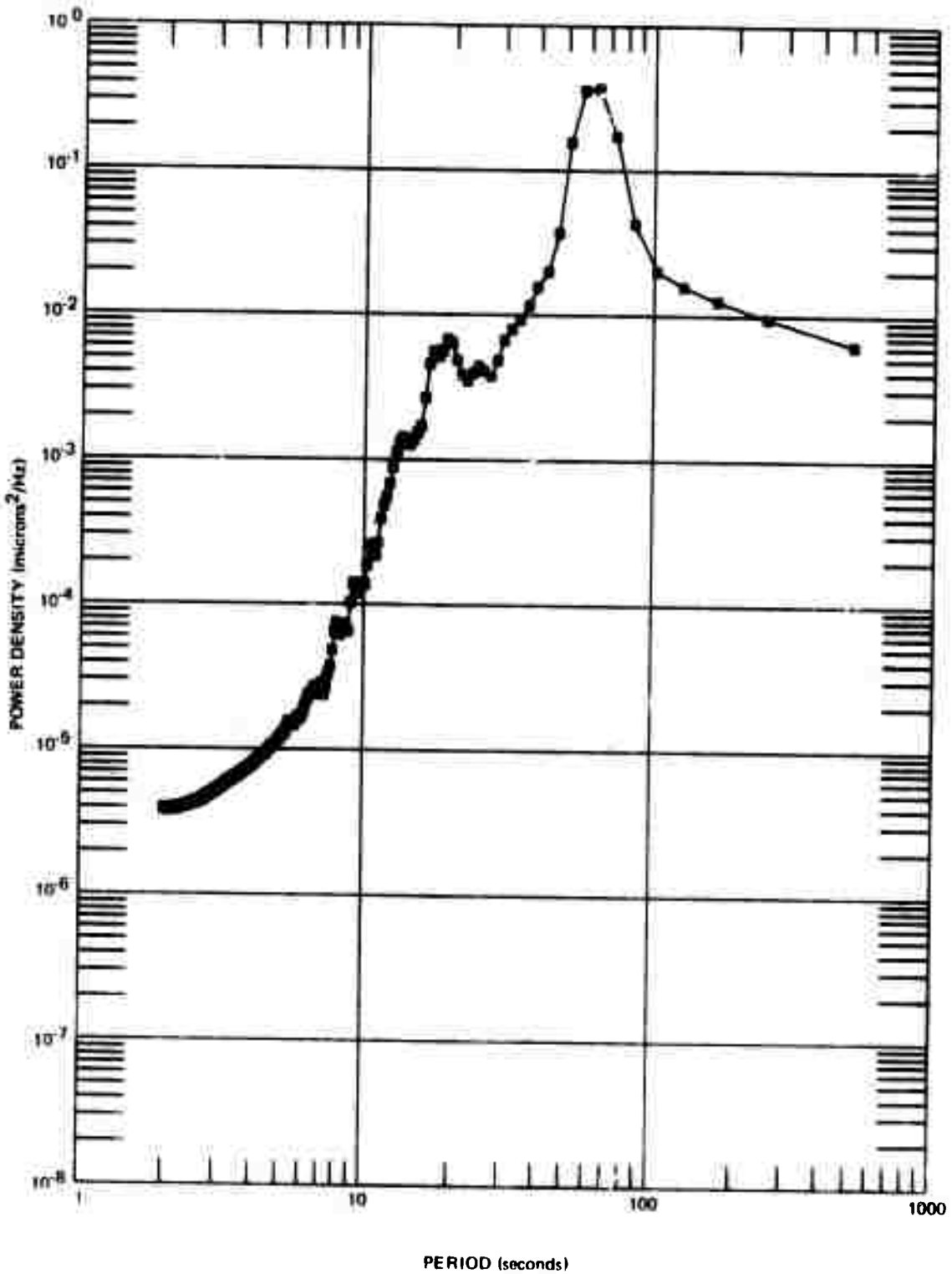


Figure 11. Power density spectrum (not corrected for response) of the noise on triaxial module TR3 during pump test

PUMP
1560 SAMPLES, 256 LAGS, 1.0 SPS, PARZEN SMOOTHING
TR2 X MKB2

FB2AK
4 MAY 1971
2121/2147

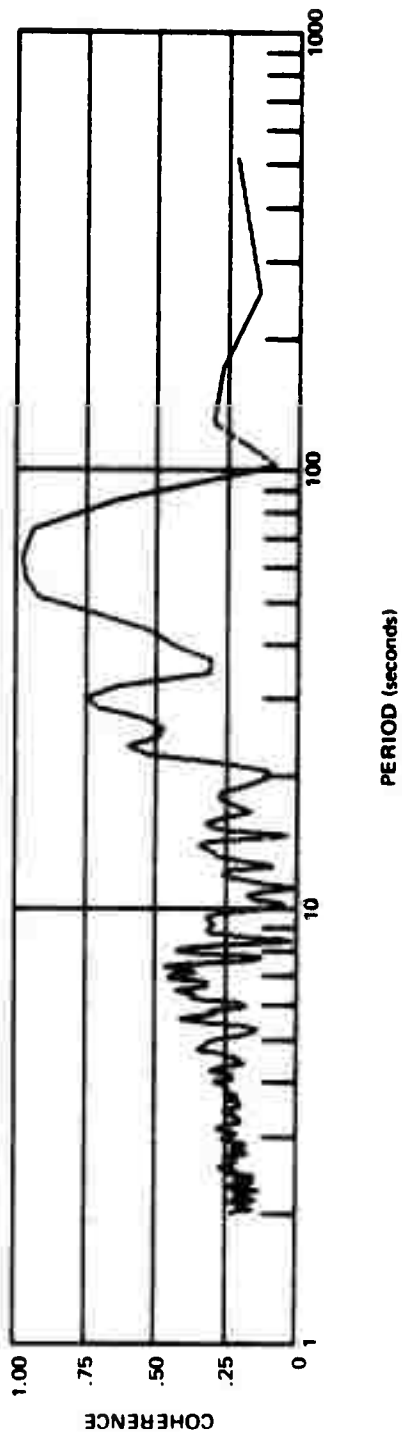


Figure 12. Coherence between the inside microbarograph and triaxial module TR2 during pump test

VACUUM
3600 SAMPLES, 256 LAGS, 1.0 SPS, PARZEN SMOOTHING
FB2AK
3 APRIL 1971
1900/2000
* TR2

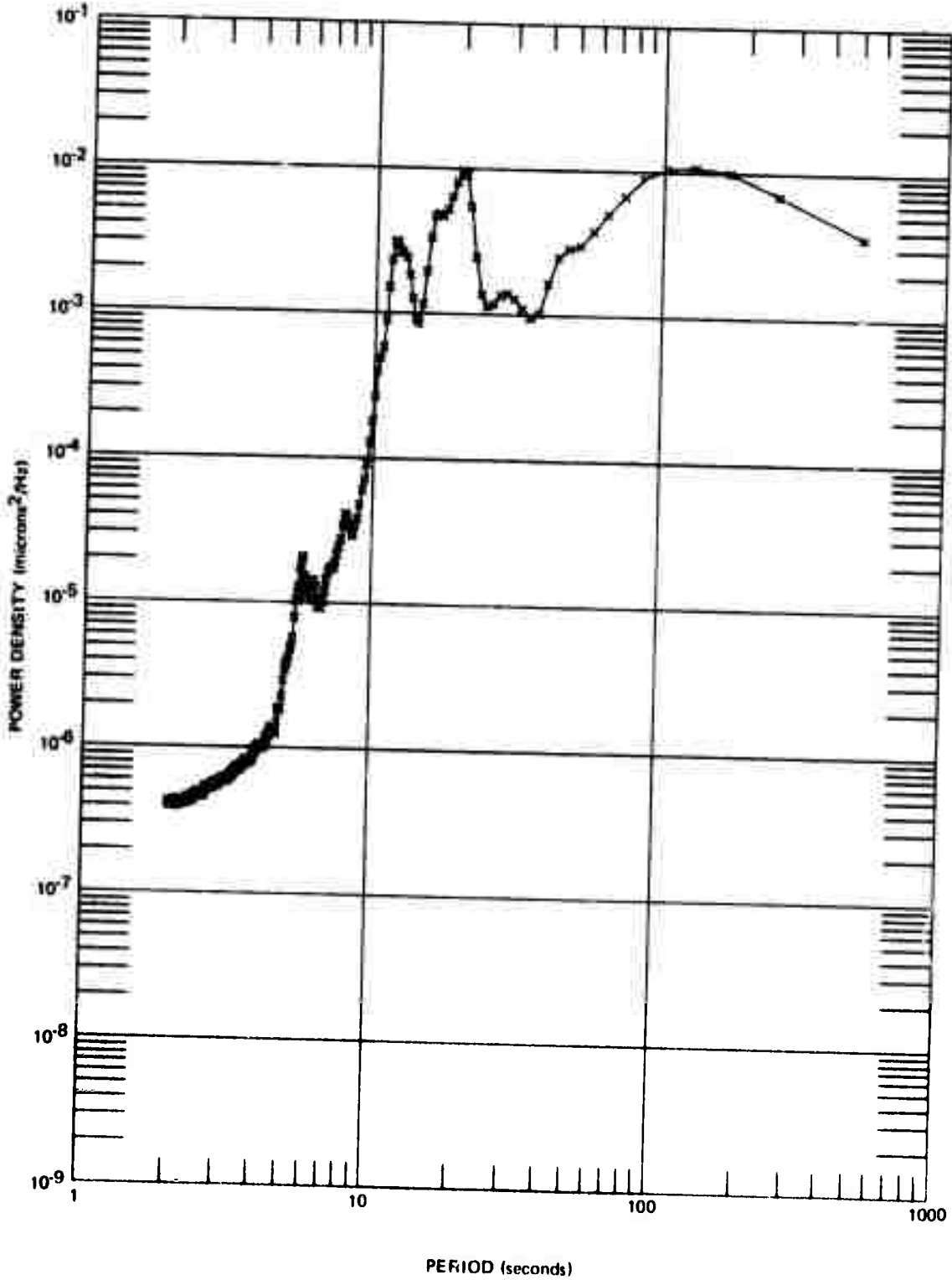


Figure 13. Power density spectrum of the noise on triaxial module TR2 during vacuum test

By letting the outside diameter of the casing approach infinity, we can compute the radial displacement for the case where the casing is perfectly cemented to the ground. The result is a displacement of 2×10^{-4} mm per μ bar.

While there is an order of magnitude difference between the two limiting cases, neither is adequate to explain the results obtained. Even changing the assumed Young's modulus by an order of magnitude does not alter the conclusion that the pressure changes are acting directly on the seismometer and not indirectly through the casing.

3.3 NOISE REDUCTION IN ALPA BOREHOLES

A brief study was made of the noise reduction that was achieved at ALPA by placing the long-period seismometers in boreholes.

Some theoretical results have been derived for the expected deformation caused by the pressure variations associated with wind-generated turbulence at the surface and at depth (Sorrells, 1970). Unfortunately, no direct information on the velocities and densities of the rocks at ALPA is available. Examination of the drilling rates of the hole at site 3-3 indicates that the rocks are quite competent, at least as compared to some of the other ALPA sites. However, the rocks are extremely fractured, therefore, the published values of elastic moduli for schists may not be applicable.

Because of the lack of information on the velocity structure at the site, it was decided to use a set of previously-computed theoretical results to try to explain the attenuation of the wind-generated noise.

Figure 14 shows the spectra of the noise recorded at the surface and in the borehole by the vertical seismographs for a wind velocity of 5 meters/second (~10 miles/hr.). Figure 15 shows theoretical vertical and horizontal surface displacements caused by wind using two different geological models. The elastic moduli used to calculate the curves shown for model 2 most closely approximate those for the rocks at site 3-3. The validity of using model 2 is confirmed by the two spectra in figure 14, which show clearly that neither of the seismographs is recording any appreciable amount of wind-generated noise even though the pressure variations at the surface were fairly constant at an rms level of between 20 and 30 μ bars. Visual examinations of other recordings made during windy periods have confirmed the spectral relationships shown in figure 14, which shows the power density of the triaxial vertical data rising rapidly at periods greater than 50 seconds and becoming greater than the power density of the surface data. It is not known whether this is caused by slight mismatch in the response curves at the longer periods or whether there is some other explanation.

5376 SAMPLES, 256 BLOCK SIZE, 0.5 SPS

FB2AK
14 APRIL 1971
0330-0630

♦ ZCT
■ LPZ

.167358315
.247556482

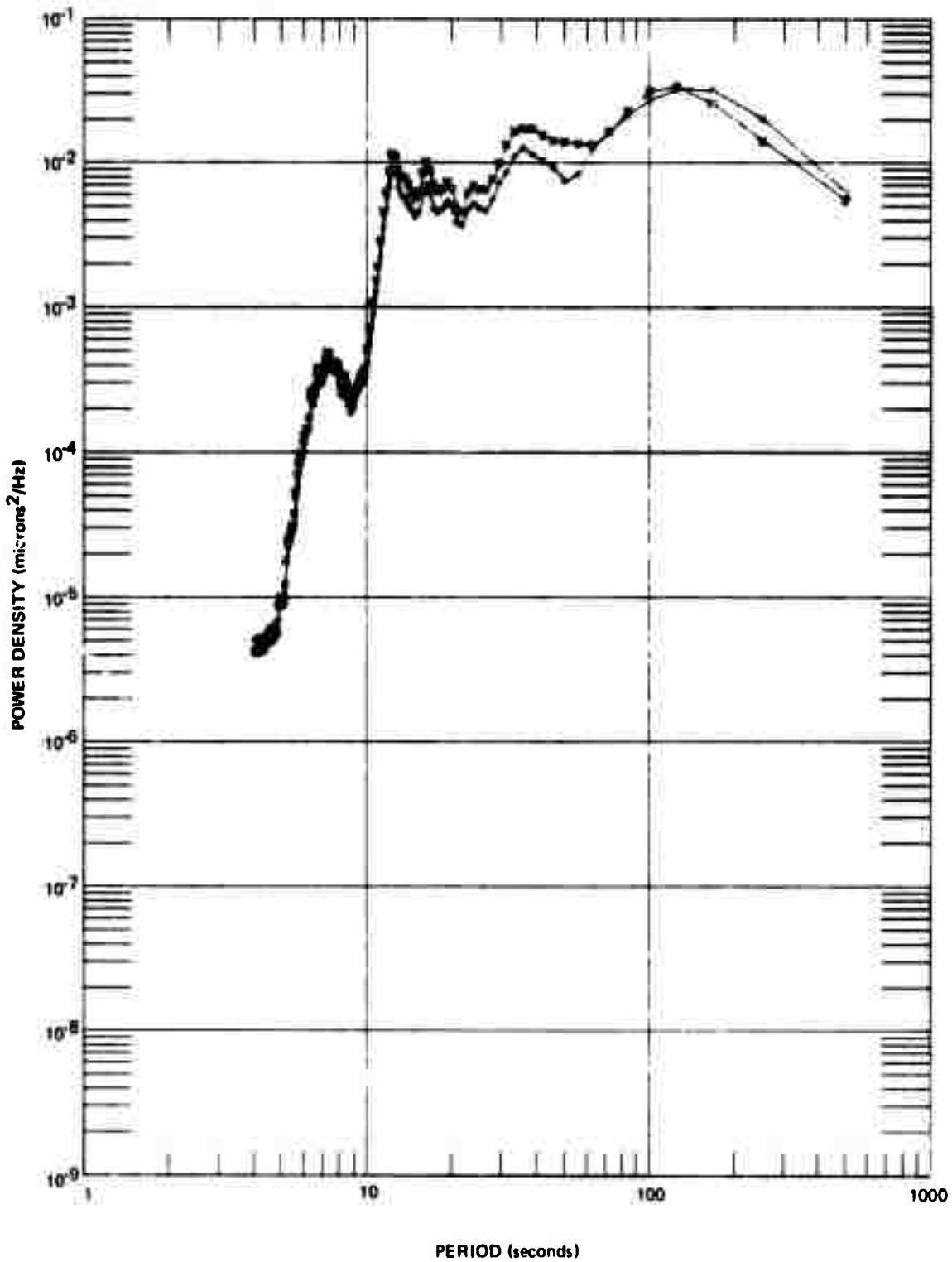


Figure 14. Spectra of the noise recorded by the surface vertical (LPZ) and the coordinate transformed vertical (ZCT) seismographs. Wind velocity 5.0 meters/sec

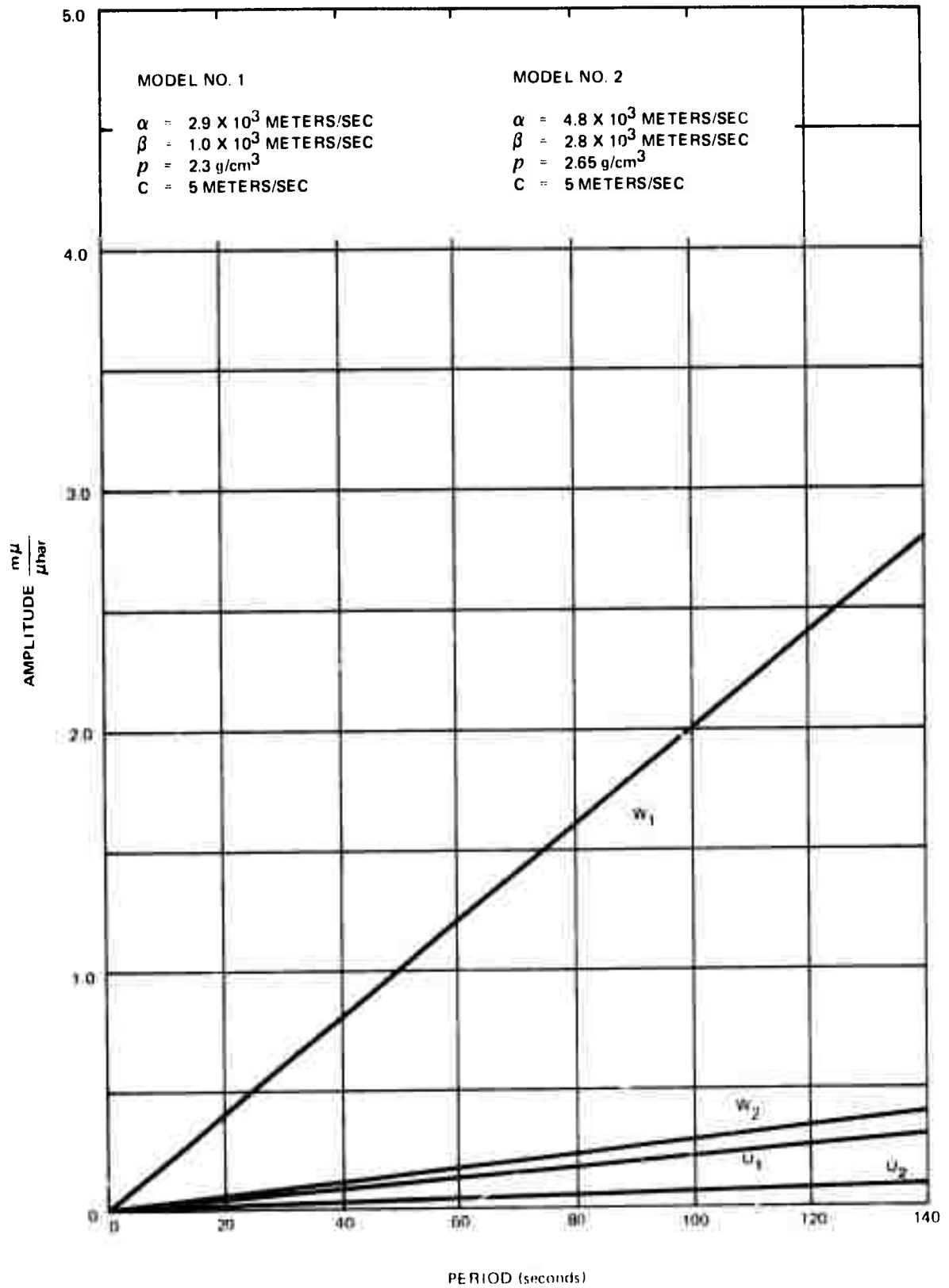


Figure 15. Theoretical vertical (W) and horizontal (U) surface displacement caused by pressure variations for a wind velocity (C) of 5 meters/sec

The coherence (figure 16) is extremely high (>0.95) for the period range where the microseisms predominate; for greater periods the coherence drops rapidly to the statistically expected zero value (0.12). Most of this lack of coherence can be attributed to the presence of system noise, but it is still surprising that the coherence decreases rapidly for periods from 30 to 50 seconds. This behavior has been noticed before, but the reason remains to be determined.

In contrast with the negligible differences between the noise spectra for the surface and triaxial vertical seismographs, there were large differences between the noise spectra for the surface and the triaxial horizontal seismographs.

Figure 17 shows the spectra of the horizontal noise obtained during the same period of time used to obtain the vertical noise spectra shown in figure 14. The higher level surface horizontal noise is predicted by the theoretical results and is caused principally by the sensitivity of long-period seismometers to wind-generated tilts. These tilts are attenuated with depth, which accounts for the noise spectra of the triaxial horizontal seismograph being lower than the surface horizontal seismograph.

The coherence between the surface and triaxial horizontals (figure 16a) is fairly low for periods outside of the microseismic band; this is typical of wind noise. The cause is probably the lack of space stationarity of the data.

As shown in figure 15, the theoretical horizontal displacements caused by pressure variations are smaller than vertical displacements. However, the pressure disturbances also produce tilts that can be a major source of noise on long-period horizontal seismographs. As shown by Sorrells² tilts are dependent on the elastic constants of the rock and on the pressure variations, but are independent of frequency. However, it has been shown that the tilt sensitivity of a horizontal seismograph is directly proportional to the square of the period. The theoretical tilts associated with a 5 meter/second wind are shown in figure 18.

As was shown by Sorrells (1970), the attenuation of tilts and vertical displacements with depth are the same and only weakly dependent on the elastic moduli. Figure 19 shows the attenuation for a halfspace. Comparing the experimental and theoretical results, it appears that the tilt attenuation obtained at 60 feet is greater than that theoretically predicted. It is probably possible to match the results by including a thin, low-rigidity layer at the surface. This would tend to give a greater tilt response at the surface and a greater attenuation with depth. The results of these tests clearly show that the susceptibility of the horizontal long-period seismograph to wind noise has been greatly reduced by burial of the seismometer at this moderate depth.

²Sorrells, G. G., Technical Report No. 70-12, Long-Period Seismic Noise and Atmospheric Pressure Variation (Teledyne Geotech, 1970)

COHERENCE **2
 5376 SAMPLES, 256 BLOCK SIZE, 0.5 SPS
 ECT X LPE

FB2AK
 14 APRIL 1971
 0330/0630

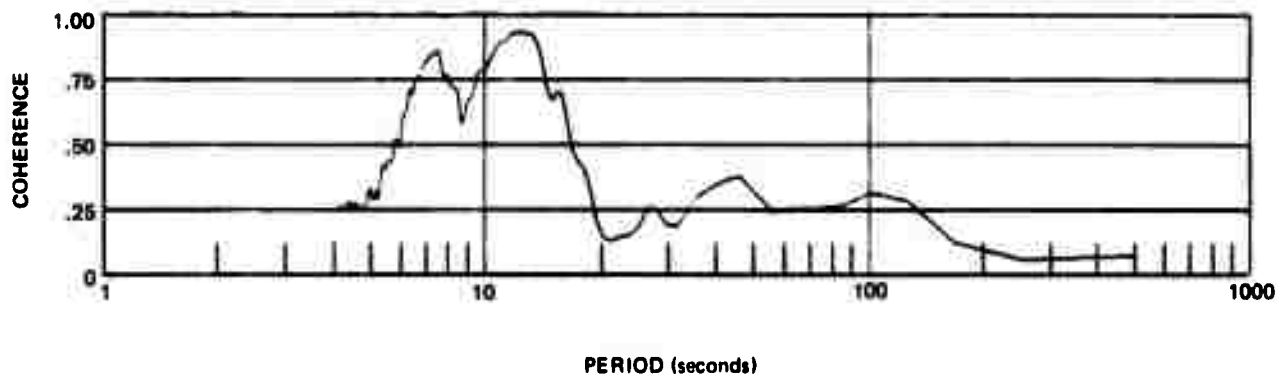


Figure 16a. Noise coherence between the east-west surface (LPE) and downhole (ECT) seismographs

COHERENCE **2
 5376 SAMPLES, 256 BLOCK SIZE, 0.5 SPS
 ZCT X LPZ

FB2AK
 14 APRIL 1971
 0330/0630

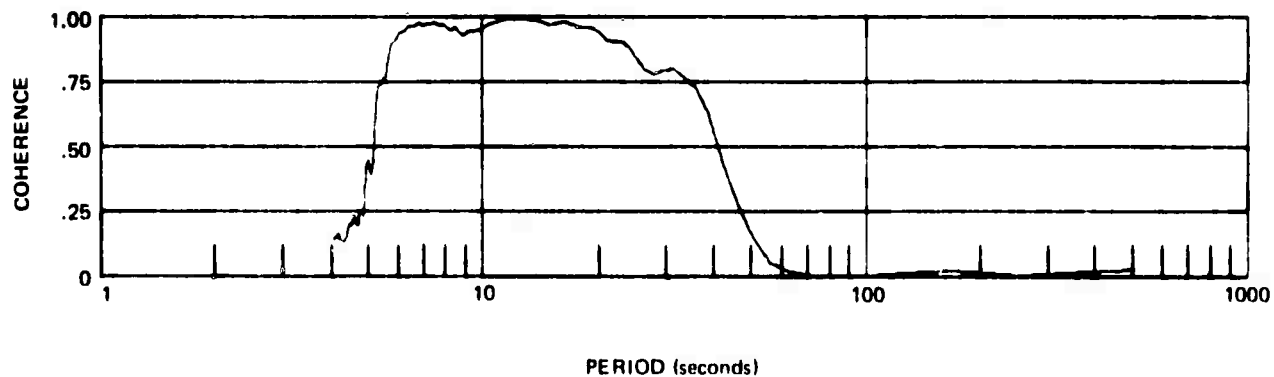


Figure 16b. Noise coherence between vertical surface (LPZ) and downhole (ZCT) seismographs. Wind 5.0 meters/sec

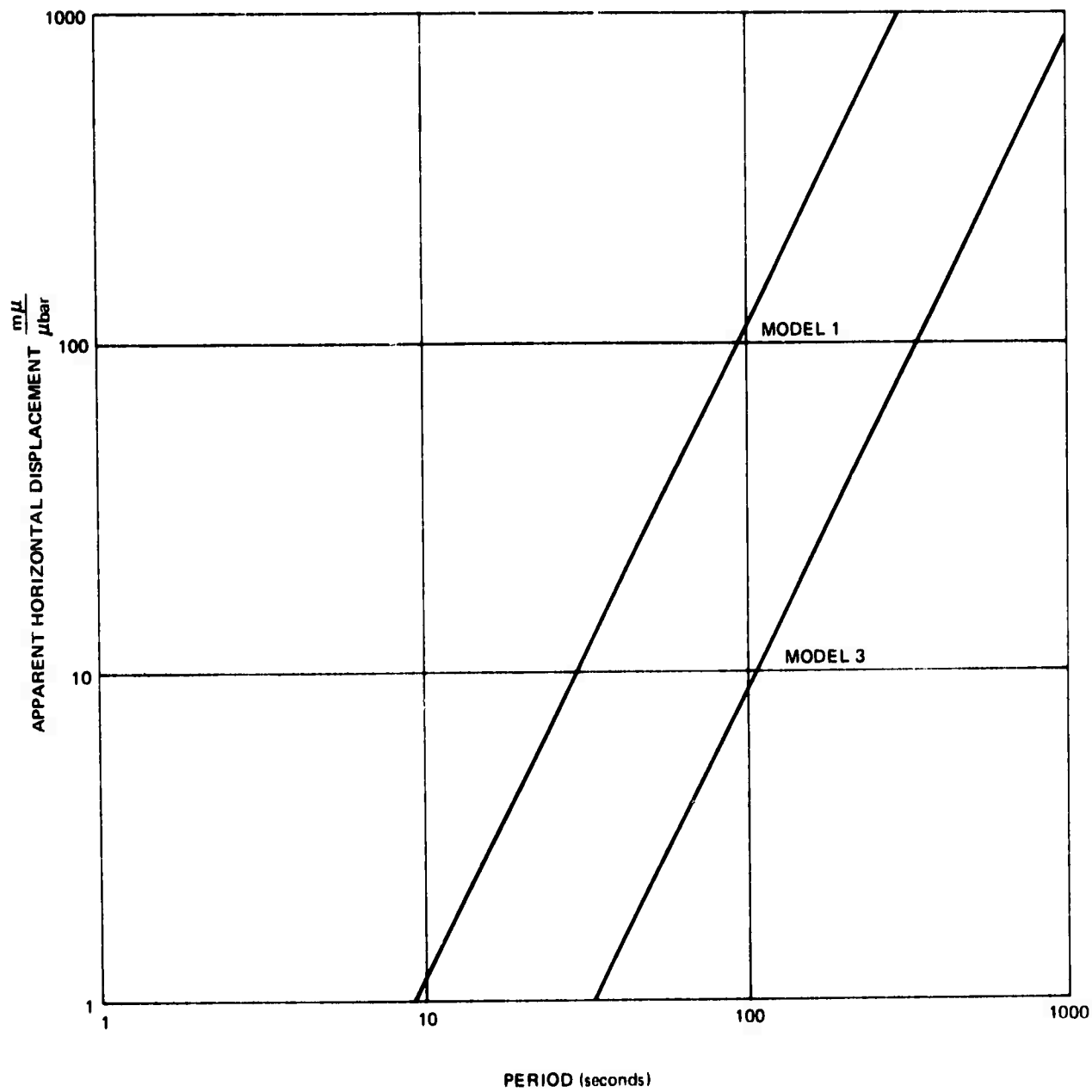


Figure 18. Theoretical apparent horizontal displacements caused by ground tilt at the free surface

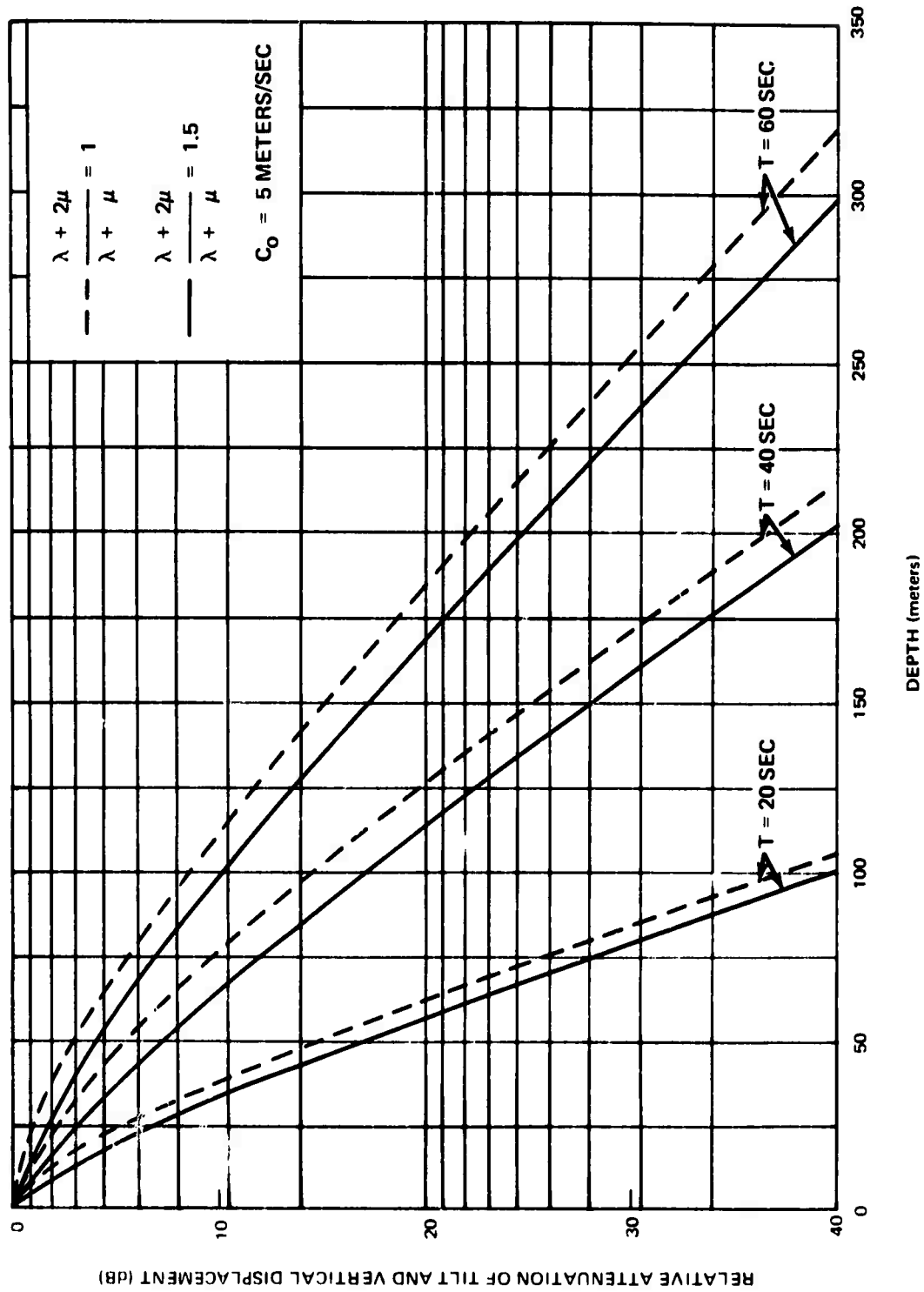


Figure 19. Theoretical attenuation of vertical displacements and tilts with depth

4. TESTS AT OTHER LOCATIONS

This section describes the tests conducted at sites other than 3-3.

4.1 TESTS AT ALPA SITE 3-34

Historically, the triaxial channel TR1 at site 3-34 has shown a higher noise level during windy conditions than have other ALPA triaxial channels. The FB2AK site personnel performed several parallel tests at this site to determine if the noise reduction techniques developed at site 3-3 would be successful in reducing this noise. These tests included: (1) filling the borehole with insulation, (2) evacuating the well, and (3) subjecting the module to pulses while the seismometer was in various orientations and anchor modes. Appendix 3 is a chronological summary of these tests.

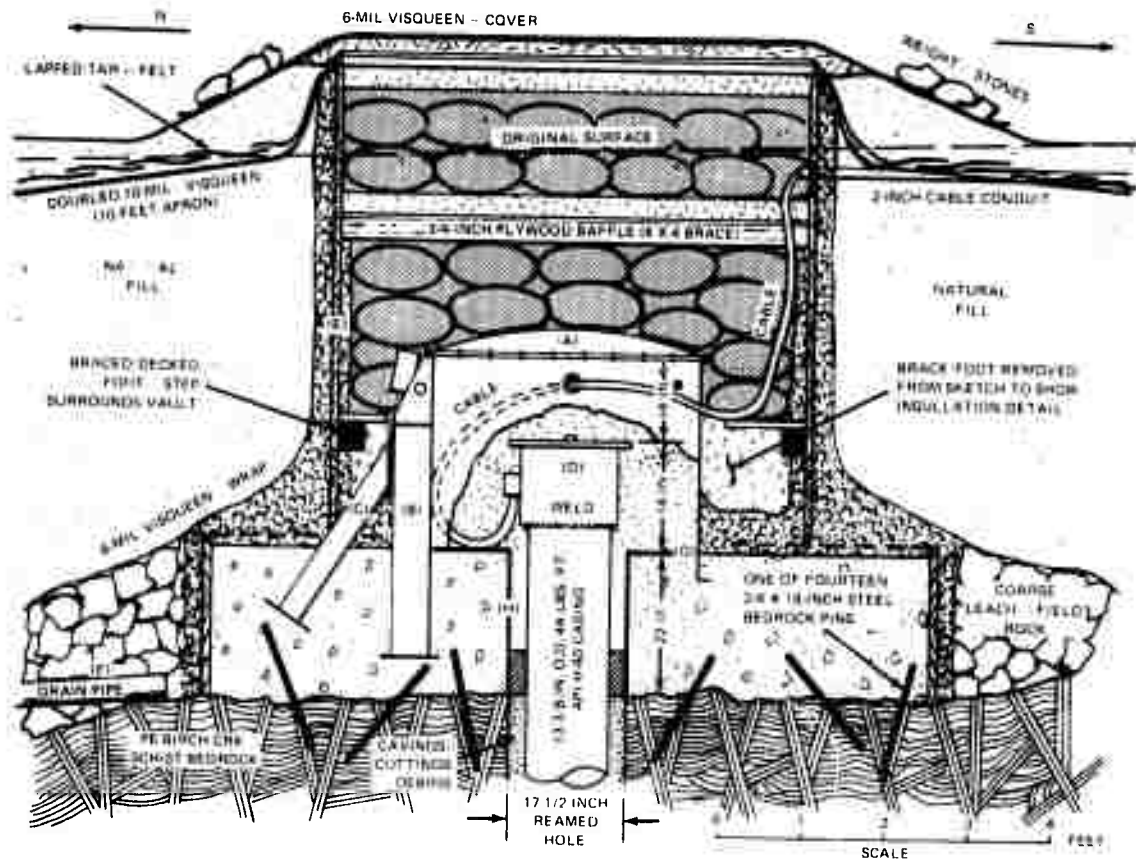
Data from these tests were transmitted via normal ALPA circuits and were unavailable for detailed analysis. However, the following general comments can be made. First, the noise on TR1 was not affected by insulation of the borehole. This suggests the existence at ALPA of another mechanism by which wind-generated noise is transmitted through the ground or casing to the triaxial seismometer. Secondly, the attempts to evacuate the borehole were only marginally successful. The best vacuum that could be achieved with equipment available for this test was 60 torr.

4.2 VAULT INSTALLATION AT ALPA SITE 2-3

Before any installation work was undertaken, the wellhead area at site 2-3 was inspected and a design for an underground vault and its installation were submitted to the Project Office. Following approval of the design, an excavation was made, the borehole casing was cut off 5 feet below the existing ground level, and a tank vault built specifically for this job was installed over the borehole. Excavation was begun on 30 March, and the installation was completed on 12 April. Figure 20 shows the tank vault and the bracing used to support the bipod assembly. Figure 21 shows a sketch of the tank installed at site 2-3.



Figure 20. Special tank vault for subsurface installation:
at ALPA site 2-3



LEGEND







- | | |
|---|--|
| <p>(A) DOMED, FLANGED, GASKETED LID OF CYLINDRICAL "MELTON-TYPE" VAULT - 10 GAUGE STEEL, 43 IN. DIA. X 33 IN. TALL, SET TO 5 IN. DEPTH IN CEMENT (W/SEALED BULK-HEAD CONNECTOR AND MICROBAROGRAPH PORT FITTINGS)</p> <p>(B) VERTICAL BRACE - 6 X 6 X 3/8 IN. 'H' BEAM W/ 10 X 10 IN. FOOT PLATE AND MILLED BIPOD SOCKET</p> <p>(C) INCLINED BRACE - 4 X 4 X 1/4 IN. 'H' BEAM W/ 10 X 10 IN. FOOT PLATE (ISOLATED FROM ENTRY BOX)</p> <p>(D) WELLHEAD COLLAR - 14.3' B IN. O.D., 12 IN. TALL, W/FLANGE FOR 1B-1/2 IN. DIA. X 3/4 IN. THICK CIRCULAR CAP (MILLED, SEALED CABLE CONNECTOR ON SIDE OF COLLAR)</p> <p>(E) ENTRY BOX AND CEMENT FORM LUMBER - PRIMARILY 2 X 12 IN. COMMON FIR, BRACED AND BOLTED W/4 X 4 IN. POSTS, PLUS 3/4 IN. THICK A/C PLYWOOD LID, BAFFLE, DECKING (WOOD PRESERVATIVE APPLIED)</p> <p>(F) DRAIN PIPE - PVC, 4 IN. DIA., 100 FT. LINEAL, PERFORATED (ALSO SECTIONS PLACED AROUND PERIPHERY OF CONCRETE PAD)</p> <p>(G) EPOXY-RESIN - 1/8 IN. THICK ON CONCRETE VAULT FLOOR (COLMA HARD SET)</p> <p>(H) ISOLATION CYLINDER - 1B IN. DIA. X 22 IN. TALL X 1/8 IN. THICK STEEL SET AROUND CASING PRIOR TO CEMENT POUR TO PROVIDE ANNULUS</p> | <p> FIBERGLASS INSULATION - PAPERBACKED, 15 IN. WIDE X 3 IN. THICK STRIPS (ALSO WRAPPED AROUND WELLHEAD AND FILLING MELTON VAULT)</p> <p> POLYSTYRENE INSULATION - LOOSE, CRUMBLED AGGREGATE FILL AROUND VAULT BENEATH STEP DECKING (8 CU. FT. VOLUME)</p> <p> POLYSTYRENE INSULATION - CRUMBLED AGGREGATE BAGGED IN PLASTIC SACKS AND FILLING ENTRY BOX ABOVE STEP DECKING (95 CU. FT. VOLUME)</p> <p> FROTHED URETHANE INSULATION - SPRAYED ON SIDE WALLS 2 X 12 BOX LUMBER, ATOP CONCRETE PAD, AND OUTSIDE FORM LUMBER (75 CU. FT. VOLUME)</p> <p> CONCRETE - 5 SACKS/CU. YD. MIX, 3/8 IN. AGGREGATE DIA., IN DIAMOND-SHAPED FORM, W/ CRUSH STRENGTH DESIGN IN EXCESS OF 3000 PSI (USED NINETY, 90 LBS/BAG 'PRE-MIX' FOR 2 CU. YDS. CEMENT VOLUME)</p> <p> ELASTIC SEALANT - 2 GALS. RTV-30 W/DEEP-CURE CATALYST NO. 9811 AND BONDING PRIMER NO. SS-4004 (G.E. PRODUCTS)</p> |
|---|--|

Figure 21. Cross-section of wellhead vault installation at ALPA site 2-3

4.3 TESTS AT THE ALPA MONITOR AND MAINTENANCE CENTER (MMC)

Tests were started using the triaxial seismometer in the unsealed borehole at the MMC, but were discontinued so that greater effort might be expended at site 3-3, where a more reliable pressure pulse generator was in operation.

4.4 TESTS AT GARLAND, TEXAS

Early pressure pulse tests at site 3-3 indicated that the pressure sensitivity of the triaxial seismograph was related in some way to the borehole configuration. Since the borehole at site 3-3 is inclined almost 2 degrees from the vertical, it appeared that this pressure sensitivity might be related to case tilt. This theory was tested at the Garland laboratory with a triaxial module fastened to a triangular baseplate placed inside a sealable tank vault. The baseplate was used to tilt the module along its sensitive axis, and a special cover was mounted on the module to seal it from external pressure changes. Pressure pulses were generated by releasing small, accurately-known volumes of air into the sealed vault. These produced repeatable pressure steps of about 0.1 psig (≈ 7 millibars).

The following steps were performed at each tilt value:

1. The baseplate was adjusted to the desired tilt;
2. The vault lid was bolted on and the vault seal was checked for a time constant of at least 5 minutes;
3. The controller was turned on and the mass was adjusted to within 1 mm of center;
4. The instrument free period was adjusted to 20.0 ± 0.5 seconds;
5. Five pressure pulses were applied.

The results of a series of tests, performed over a 2-month period, are plotted in figure 22. Although high ambient noise levels and discontinuous test performance caused some data scatter, the plots appear to demonstrate a relationship between module tilt and pressure sensitivity. The first series showed that the pressure sensitivity varied by a factor of almost three for a forward tilt of just under 1/2 degree. The second series, in which the module is leveled, shows that the data are repeatable. The last two series show that the pressure sensitivity reaches a maximum at about 20 minutes of backward tilt and then decreases with additional backward tilt. In all cases, the seismogram trace deflection was mass down for positive pressure. Note this polarity is opposite from that which would be produced by mass buoyancy.

In another test, the module was mounted in a level position, and its pressure sensitivity as a function of free period was measured. The test results, plotted in figure 23, show that the pressure sensitivity increases with increasing period when all other parameters are held constant.

BACKWARD (-) TILT FORWARD (+) TILT

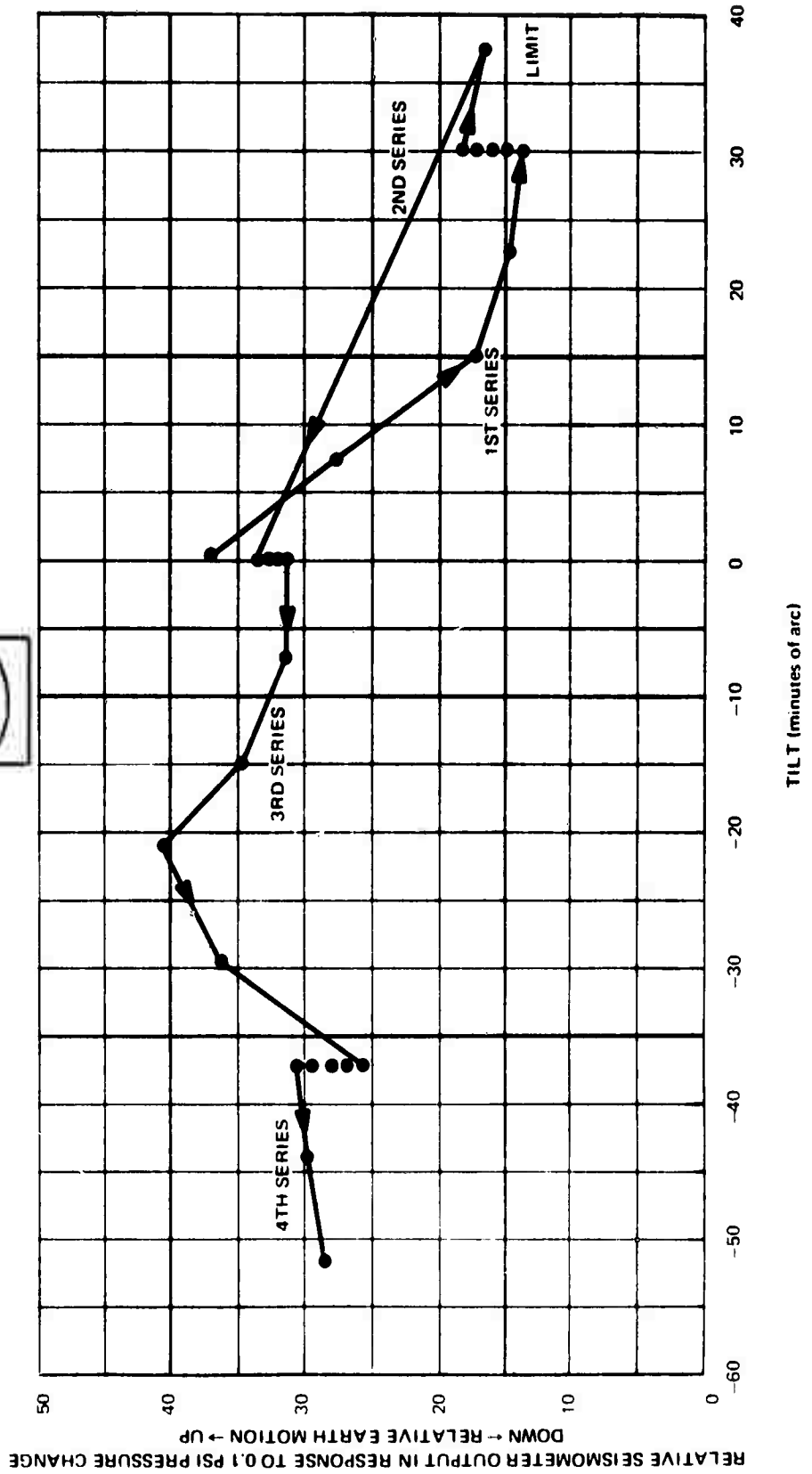
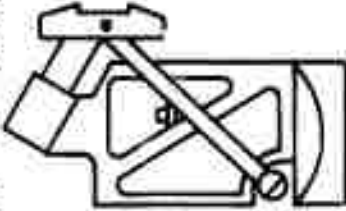


Figure 22. Pressure sensitivity of triaxial seismometer module as a function of module tilt. Free period adjusted to 20 ± 0.5 sec for each data point

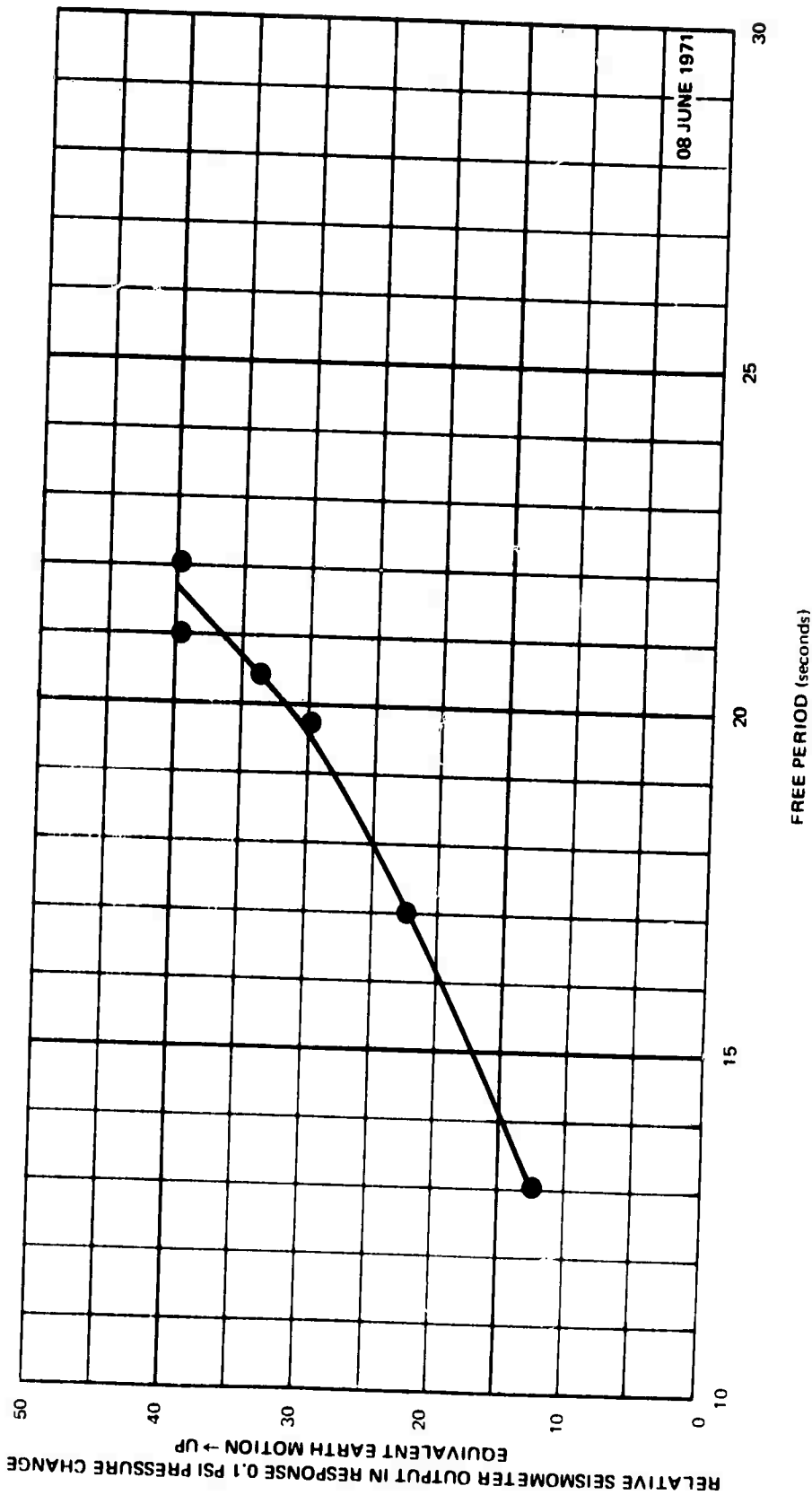


Figure 23. Pressure sensitivity of triaxial seismometer module as function of module free period

5. CONCLUSIONS AND RECOMMENDATIONS

Results of the tests conducted at ALPA indicate that convection cells in the boreholes are the most likely cause of the 50-60 second noise recorded during the winter months, and that air baffling in the borehole will prevent the formation of these cells. It is recommended that the air-baffles be installed in selected ALPA boreholes for operational tests during the coming winter months.

It was concluded that triaxial seismometer modules operated at depth in sealed boreholes, responded significantly less strongly to wind-generated horizontal seismic noise than did surface seismometers.

Although field tests demonstrated that module pressure sensitivity is related, in some way, to the manner in which the instrument is installed in a borehole, and laboratory tests demonstrated that a relationship exists between pressure sensitivity and module tilt, little is known about the mechanism that causes the module to produce outputs in response to air pressure changes. It is recommended that studies be undertaken to learn more about triaxial module pressure sensitivity, and its relationship to installation techniques, environmental conditions, and module construction. Information from these studies should aid in the development of instrument and installation technique modifications for reducing spurious responses of the triaxial seismograph.

APPENDIX 1 to TECHNICAL REPORT NO. 71-22

SUMMARY OF TRIAXIAL SEISMOMETER TESTS AT FAIRBANKS, ALASKA,
ALPA SITE 3-3

SUMMARY OF TRIAXIAL SEISMOMETER TESTS AT FAIRBANKS, ALASKA,
ALPA SITE 3-3

March - June 1971

<u>Date</u>	<u>Test</u>	<u>Conditions</u>	<u>Results</u>
8 March	Pressure pulses at standard orientation	-12 to -30°F; winter noise evident	TR1, -32 mm; TR2, +40 mm; TR3, -25 mm. Same phase as winter noise
11 March	Pressure pulses at 120° CCW rotation	-6 to -28°F; winter noise	TR1, +52 mm; TR2, -31 mm; TR3, -52 mm. Same phase as winter noise
13, 14 March	Pressure pulses at 240° CCW rotation	0 to -18°F	Data unreadable - too much noise and overlining
17, 18 March	Pressure pulses at standard orientation	+40 to +20°F (data 12 dB down)	TR1, +70mm; TR2, -70 mm; TR3, +36 mm
29 March	Well evacuated to 4 torr	+20 to 0°F light winds	Wind generated noise on triax correlates with surface data. No rise in noise level with decrease in well-head temperature
30 March	Dry ice - no vacuum	+20 to 0°F	TR1 & 3 large and out of phase. TR2 quiet
31 March	Dry ice on wellhead; vacuum at 17 torr	+20 to 0°F wind low to calm	Noise decreases considerably with increase in vacuum
1-4 April	Vacuum held at 4 torr	+32° to -10°F (max) High winds 1 & 2 April, low to calm winds 3 & 4 April	LP tilt due to high wind on triax
10 April	MKB #2 in operation to sense well pressures; upper bore-hole thermistor on	+18 to -3°F	Data from MKB #2 visually correlate with triax data. Noise on MKB #2 trace increases as temperature goes down at night.

<u>Date</u>	<u>Test</u>	<u>Conditions</u>	<u>Results</u>
11 April	Pressure pulses standard orientation	20 to -5°F	TR1, no response; TR2, -41 to 26 mm; TR3, -81 to 55 mm. (4 pulses - amp varies)
13 April	Dry ice on well-head	46 to 30°F	30 to 50 μ bar avg, >125 μ bar p-p - 3 triax in phase, TR1 \approx 4 mm, TR 2 \approx 20 mm, TR3 \approx 30 mm
14 April	Well filled with shredded styro-foam insulation; sealed	46 to 31°F	All triax quiet - LP component
20 April	Well unsealed, but filled with insulation	40 to 24°F	MKB #2 shows 10-20 μ bar p-p @ low wind. TR responds as with dry ice on 13 April; much lower amplitude. Wind loading also contributes - TR1 out of phase with TR2 and TR3.
25 April	3 feet insulation removed from bore-hole, sealed. Dry ice on wellhead	50 to 35°F	MKB #2 shows 30-50 μ bar avg, \approx 100 μ bar max; TR1 out of phase with TR2 & TR3
29 April	(1) Pressure pulse with insulation	40 to 20°F	TR1, +22 mm; TR2, -43 mm; TR3, -53 mm
	(2) Well unsealed & filled to within 3 feet of top with insulation	40 to 20°F	Approx. 10-15 μ bar on MKB #2; too small to see on triax
30 April 3 May	Routine recording with all insulation out of well	50 to 26°F (max)	See triax respond to pulses greater than \approx 25 μ bar
4 May	Sine wave pressure pump on wellhead	40°F	21 μ bar p-p @ 60 sec TR1, 3 mm @ 90° lag; TR2 and TR3, 5 mm @ 270° lag

<u>Date</u>	<u>Test</u>	<u>Conditions</u>	<u>Results</u>
4-12 May	Stiffener Installation		
	NOTE: During this time, input part for MKB #2 was moved from top of well to a point near top of triax.		
13 May	Pressure pulses; stiffener on, triax on bottom; no insulation	55 to 40°F	TR1, -30 mm; TR2, -33 mm; TR3, -13 mm
15 May	Dry ice on wellhead	45 to 30°F	MKB #2, 50-60 μ bar avg; 300 μ bar, max. All triax in phase and \approx 270° lag from MKB #2; relative amplitudes -TR1, 55 mm; TR2, 50 mm; TR3, 19 mm
	NOTE: Input for MKB #2 moved to top of borehole on 18 May.		
19 May	Pressure pulses; stiffened triax on holelock and stabilizer	52 to 40°F	TR1, -33 mm; TR2, -35 mm; TR3, -20 mm
21 May	(1) Pressure pulses; still on holelock stabilizer retracted	60 to 40°F	TR1, -27 mm; TR2, -38 mm; TR3, -27 mm
	(2) Pressure pulses; triax rotated 120° CCW and on bottom	60 to 40°F	TR1, -38 mm; TR2, -41 mm; TR3, -44 mm
23 May	(1) Pressure pulses triax rotated 240° CCW and on bottom	58 to 38°F	TR1, -55 mm; TR2, -42 mm; TR3, -28 mm
	(2) Sine wave pressure pump on well		All triax respond in phase
24-26 May	Routine operation at standard triax orientation	-	-

<u>Date</u>	<u>Test</u>	<u>Conditions</u>	<u>Results</u>
27 May	Triax rotated 240° CCW from standard	40 to 60°F	
28 May	Triax at 240° CCW orientation - stabilizer re- tracted	35 to 50°F	
29 May - 4 June	Triax off to seal stiffener		
NOTE: During this time, upper triax module (TR3) found to be leaking through downhole data cable. Corrected. Other modules found pressure-tight.			
6 June	Pressure pulses at standard orientation	≈ 80°F	TR1, -58 mm; TR2, -8 mm; TR3, +20 mm
7 June	(1) Sine wave pres- sure pump on well	≈ 75°F	Pump produces ≈ 90 μbar, p-p - TR1 & TR3 respond, out of phase; TR2 response not evident
	(2) Triax tilt test with surface loading (drive truck to well)	Approach from south	TR1 pos, TR2 & TR3 negative. Little vertical motion on ZCT
		Approach from east	TR1 & TR3 approx. equal and out of phase. Little or no response from TR2 or ZCT.
8 June	Pressure pulses at standard orientation	≈ 68°F	TR1, -58 mm; TR2, -11 mm; TR3, +22 mm
9 June	(1) Pressure pulses at standard orientation	≈ 65°F	TR1, -55 mm; TR2, -8 mm; TR3, +18 mm
	(2) Pressure pulses at standard orientation; on holelock	≈ 65°F	TR1, -43 mm; TR2, -12 mm; TR3, +27 mm

<u>Date</u>	<u>Test</u>	<u>Conditions</u>	<u>Results</u>
10 June	Pressure pulses at 120° CCW orientation; on bottom	~ 80°F	TR1, -31 mm; TR2, -12 mm; TR3, +22 mm
12 June	Pressure pulses at 120° CCW orientation; on holelock	~ 60°F	TR1, -35 mm; TR2, -12 mm; TR3, +22 mm
14 June	Roll-up		

NOTE: All deflections read from
film at X20 view; triax gains
28K to 30K; readings are un-
corrected for instrument
response.

APPENDIX 2 to TECHNICAL REPORT NO. 71-22

RESPONSES OF TRIAXIAL SEISMOMETER MODULES
TO PRESSURE PULSES

RESPONSES OF TRIAXIAL SEISMOMETER MODULES
TO PRESSURE PULSES

<u>Date</u>	<u>Equivalent ground motion in microns</u>			<u>Surface air temperature in of</u>		<u>Site</u>	<u>Comments</u>
	<u>TR1</u>	<u>TR2</u>	<u>TR3</u>	<u>Low</u>	<u>High</u>		
8 Mar 71	-2.20	+2.67	-1.67	-30	-12	3-3	Direct 0° winter noise noted
11 Mar 71	+3.46	-2.06	-3.46	-28	-6		120° CCW winter noise noted
13 Mar 71				-18	0		240° CCW too noisy
17 Mar 71	+4.66	-4.66	+2.40	20	40		0° No winter noise
11 Apr	-	-2.30	-4.53	-5	20		0°
29 Apr	+1.47	-2.87	-3.54	20	40		0° Filled with crumbled polystyrene
13 May	-2.76	-2.20	-0.87	40	55		0° Stiffener on triax, triax or bottom
19 May	-2.20	-2.33	-1.33	40	52		0° Stiffener with holelock and stabilizer
21 May	-1.80	-2.53	-1.80	40	60		0° Stiffener, with holelock
21 May	-2.53	-2.73	-2.83	40	60		120° Stiffener, no holelock, no stabilizer
23 May	-3.66	-2.80	-1.80	38	58		240° Stiffener, no holelock, no stabilizer
6 June	-3.86	-0.53	+1.33	~ 80			0° Stiffener sealed
8 June	-3.86	-0.74	+1.47	~ 68			0° Stiffener sealed
9 June	-3.67	-0.53	+1.20	~ 65			0° Stiffener sealed
9 June	-2.86	-0.80	+1.80	~ 65			0° Stiffener sealed on holelock
10 June	-2.07	-0.80	+1.47	~ 80			120° Stiffener sealed on bottom
12 June	-2.33	-0.80	+1.47	~ 60			120° Stiffener sealed on holelock

APPENDIX 3 to TECHNICAL REPORT NO. 71-22

SUMMARY OF TRIAXIAL SEISMOMETER TESTS AT ALPA SITE 3-34

SUMMARY OF TRIAXIAL SEISMOMETER TESTS AT ALPA SITE 3-34

15 April Baffle installed on top of triax and borehole filled with insulation

17 May Removed insulation and baffle

18 May Well evacuation in progress; 170 torr at 0400Z;
120 torr at about 1900Z (generator stopped)

19 May Well evacuation in progress
>200 torr start of run (generator stopped);
60 torr at 1900 (generator running)

20 May a. Well evacuation in progress
60 torr at 0300 (generator running);
>200 torr at 1800Z (generator stopped)
1802Z - released vacuum

 b. Rotate stack 90° ccw and resume operation at
2330Z.

25 May Pressure pulses (2300Z to 2325Z)

26 May a. Rotate stack to 180° ccw orientation and resume operation
0045Z

 b. Pressure pulses (0050Z to 0055Z)

16-17 June Install holelock on stack